EUROPEAN ORGANIZATION FOR NUCLEAR RESEARCH

NPA/Int 69-16
19 September, 1969.

THE MAGNETIC FIELD OF THE 1.1 m^3 CERN HEAVY-LIQUID BUBBLE CHAMBER

R. Grüb and B. Langeseth

SUMMARY

To increase the rate of neutrino interaction data-recording, the CERN Heavy-Liquid Bubble Chamber has been enlarged to a volume of more than 1.1 m^3. The new characteristics of the magnetic field are described, together with some technical details of the magnet. (This is a re-issue of a note made following the modifications done in 1964.)

CONTENTS

1. INTRODUCTION

In order to increase the rate of data collection in the CERN neutrino experiment and to save PS machine time, the 500 litre heavy-liquid bubble chamber[1,2] has been enlarged to a volume of more than 1.1 m^3. Many of the main components had to be replaced or modified. This report describes the new characteristics and some constructional details of the magnet. The modification of the magnet involved both the addition of new windings and the extension of the steel parts of the magnetic circuit, as well as a few minor changes found useful after some years of practical experience. As a result of careful following-up, the modification could be completed according to a very tight time-schedule, and the magnet was out of service for less than 5 months. In all, it took only 12 months from the final decision to start the project until tracks were photographed in a 2.7 Wb/m^2 field in the new chamber. The complete chamber assembly and the magnet are shown in Figs. 1 and 2, respectively.

2. THE MAGNETIC FIELD

2.1 Coordinates and definitions

The coordinates used for defining the magnetic field direction at any point are shown in Fig. 3. The symbols used in the text and graphs have the following meaning:

i) T_0, R_0, Z_0: coordinates, see Fig. 3;

ii) B_{0z}: z-component of the magnetic flux density at the origin;
B_r : radial field component;

iii) I : excitation current.

2.2 Measuring methods

Preliminary field maps were obtained from measurements on analogue models assuming infinite permeability of the steel. The lower part of the magnetization curve was measured with a nuclear resonance magnetometer. At higher fields the measurements were made with a Hall-effect magnetometer, since the field uniformity was insufficient for obtaining a good resonance signal. The field mapping throughout the volume of the chamber was also made with the same Hall-effect magnetometer, accurately calibrated

against a nuclear resonance reference before and after the measurements. The Hall current and Hall voltage were measured with a precise digital voltmeter (five digits), while the magnet current was measured with the shunt and digital voltmeter (three digits only) used under normal service conditions.

2.3 The magnetization curve

The magnetic flux density in the middle of the chamber as a function of current is shown in Fig. 5. It is noted that a 50% increase in power consumption from 3 to 4.5 megawatt gives an increase of nearly 20% in the magnetic flux density.

The magnetization curve as well as the spatial distribution may possibly be affected by large quantities of steel placed close to the magnet (e.g. for cosmic-ray shielding).

2.4 The magnetic field distribution

The magnetic field distribution throughout the chamber volume is shown in Fig. 6. At the front end (the camera side of the chamber) the magnet is open except for the steel parts of the safety tank, and the field distribution is similar to that of an air core magnet. At flux densities higher than 2.0 T this tends to become the case also for other regions of the field.

A somewhat better field could possibly be achieved by modifying the rear plate.

The field direction is fairly parallel with the chamber axis except at larger radii near the glass window. The worst deviation inside the chamber volume is about 250 milliradians, and considerably less inside the fiducial volume.

3. CONSTRUCTION DETAILS AND TESTING

3.1 The excitation coils

The windings are divided into two groups separated by a space of about 20 cm so as to leave a free passage for particles entering the chamber through the beam window as shown in Figs. 1, 2, and 3.

The axial layers each having 14 turns are assembled in pairs or double pancakes by brazing together the ends of the two inner turns of each pair. Each double pancake is insulated and impregnated as a separate unit. There are 17 of these coil elements and all are connected in series electrically. Each double pancake has two parallel cooling water circuits, one for each layer. The water enters at the outer turn of each spiral and leaves at the inner junction of each double pancake.

The conductor is made of copper of rectangular cross-section with a circular cooling water channel in the middle.

Further data are listed in Table 3.

The insulation both of individual conductors and of each double pancake assembly consists of several layers of fibre-glass reinforced mica tape. Each double pancake is vacuum impregnated with a low viscosity epoxy compound. This is the standard type of insulation adopted in our specifications since many years, and the quality is tested by 5000 volts under water after immersion for 24 hours, as described later in this section.

3.2 The magnetic circuit

The geometry of the steel parts of the magnetic circuit is shown in Figs. 1, 2, and 3. Two thick end plates are bolted together with the return circuit consisting of two side plates, a top plate, and a thin base plate. The central region of the rear plate is an integral part of the chamber, and is detachable from the magnet together with the chamber assembly.

The steel parts of the safety tank have a small but noticeable effect on the magnetic field inside the chamber.

The chemical composition of the steel parts is given in Table 4.

3.3 Tests and inspections

High reliability is required for ensuring safe operation, especially when the chamber is used with liquids that may form inflammable mixtures with air. Detailed tests were therefore specified for the various components and production processes of the magnet, and frequent inspections were made to verify the standards of workmanship maintained as well as the rate of progress.

The more important tests and checks are summarized in the following list:

i) Dimensional checks of the copper conductors. A 15 mm diameter steel ball was blown through the water channel of each length of conductor.

ii) Measurements of mechanical properties and resistivity of the copper conductor material.

iii) X-ray radiographic checks of some of the brazed joints of the conductor. Before insulating the conductor, each brazed joint was bent and straightened again in two mutually perpendicular planes, and then subjected to a tensile force of 5 tons and a pressure test.

iv) Dimensional checks of each impregnated double pancake. Flatness and uniformity of thickness combined was required to be better than ±0.5 mm.

v) Measurement of water flow as a function of pressure difference.

vi) Thermal cycling test, 10 cycles of a temperature variation of 75°C of the outlet water.

vii) Leak test, 80 kg/cm^2 for 24 hours after purging thoroughly with hot water.

viii) Insulation to ground of each double pancake. After immersion in tap water for 24 hours, 5000 volts r.m.s. was applied between the conductor and the water for 1 minute. Insulation resistance was measured before and after each stage of the testing.

ix) Inter-turn insulation was tested by 2400 volts r.m.s. applied between the terminals of each double pancake for one minute.

x) Testing of assembled magnet at normal service condition for two hours with cooling water adjusted for an outlet temperature of 70°C, followed by an insulation test of 5000 volts r.m.s. for one minute between the yoke and the coil terminals, and measurements of the insulation resistance between the same points.

4. POWERING AND COOLING, MONITORING AND PROTECTION

The original magnet current supply sets available for track chamber magnets in the CPS experimental areas were composed of modules rated 600 V 2500 A, and the magnet parameters are matched to three of these modules in parallel, 600 V 7500 A. The magnet current is measured with a shunt and a digital voltmeter, and the reading can be recorded on each particle track photo. The stability of the current should normally be within 0.1% over a few hours.

Demineralized cooling water is supplied to the experimental area at a pressure of 15-25 kg/cm^2 and a temperature of 20-30°C. At normal service condition, a waterflow of 100 m^3/h corresponds to a temperature increase of about 40°C of the cooling water. The water outlet temperatures of the two parallel water circuits of each double pancake are measured with resistance thermometers mounted at each outlet.

Bimetal switches are mounted directly on the copper conductor, both at the outlet and the inlet end of each cooling circuit in order to provide protection against overheating. A waterflow switch is mounted in each water circuit, and the contacts are interlocked with the regulator of the magnet current supply.

Acknowledgements

The realization of the equipment is the result of the joint effort of several members of the Nuclear Physics Apparatus Division under the direction of Dr. C.A. Ramm.

The original chamber was designed and constructed under the responsibility of L. Resegotti, and the manufacturing and testing of the original magnet was supervised by S. Pichler. P.G. Innocenti was, before leaving, responsible for the initial phases of the present modification, and the main co-ordination of the work was continued by Ch. Scherer. All detailed design and checking of contractor's drawings were made by J.J. Hirsbrunner and his colleagues of the NPA Drawing Office. P. Actis took care of the magnet protection circuits.

Acknowledgement is due to S. Pichler for useful information about the original magnet, and to R. Gerst who participated in the magnetic measurements as well as the tests and inspections during the manufacturing of the magnet.

REFERENCES

1) C.A. Ramm and L. Resegotti, The principles of the design of the CERN propane bubble chamber, Proc. Int. Conf. on High-Energy Instrumentation, Berkeley (1960).

2) S. Pichler and G. Pluym, Measurements of the magnetic field of the heavy-liquid bubble chamber magnet, CERN internal report NPA/Int. 62-2, 15 March 1962.

Table 1 : Magnetic field data

Magnetic flux density at 7500 A	2.65 Wb/m^2
Magnetic flux density at 5000 A	1.95 Wb/m^2
Field error along axis	+3% -27%
Integrated fringing field in beam window at 7500 A	0.7 Wb/m

Table 2 : Physical dimensions and weights

Height of magnet axis (beam height)	1.240 m
Total weight	96 ton
Weight of coils	17 ton
Weight of magnetic circuit	79 ton
External height	2.690 m
External width in beam direction	3.150 m
External length approx.	2.5 m
External length without water manifolds, etc.	2.153
Free internal diameter	1.4 m
External coil diameter	2.4 m
Thickness of double pancake	64.2 ± 0.5 mm

Table 3 : Electrical parameters and coil data

Coil resistance at 20°C, R_{20}	0.0743 Ω
Excitation current (nominal), In	7500 A
Voltage drop, In R_{20}	560 V
Power loss, In^2 R_{20}	4.2 MW
Magnetic energy	10 MJ

Coil data

Total number of turns	476
Number of double pancakes 9 front + 8 rear =	17
Turns per double pancake 14 + 14 =	28
Conductor cross-section 30 × 30 mm - 18 mm diameter hole =	645 mm^2
Water channel cross-section 18 mm diameter	245 mm^2

./.

Coil data (continued)

Water flow at 20°C and 6 kg/cm^2 pressure drop	100 m^3/hour
Test voltage between coil and yoke	5000 V r.m.s.
Interturn test between terminals of each double pancake	2500 V r.m.s.
Insulation test of each double pancake against water after 10 thermal cycles and 24 hours immersion in water	5000 V r.m.s.

Table 4 : Magnetic steel data

Element	Percentage
Carbon	0.11
Silicon	0.42
Manganese	0.58
Phosphorus	0.013
Sulphur	0.020

Magnetic flux density at 3.10^4 A/m: 2.05 Wb/m^2

Table 5 : Parameters of available power supplies

I_{max}	3 × 2500 A	7500 A
V_{max} at I_{max}		600 V
I_{max} V_{max}	3 × 1.5 MW	4.5 MW
V_{max}/I_{max}		0.080 Ω
Current stability over 24 hours, approx.		0.1%
Cables 2 × 20 cables, each 240 mm^2		2 × 4800 mm^2
Current measuring shunt		50 μΩ

Figure captions

Fig. 1 : The 1.1 m^3 chamber assembled in the magnet.

Fig. 2 : Photographic view of the 1.1 m^3 chamber.

Fig. 3 : Reference frame.

Fig. 4 : Photographic views of the magnet.

Fig. 5 : Magnetization curve.

Fig. 6 : Axial flux density along the Z-axis.

Fig. 7 : Example of two-dimensional analogue measurement of field distribution.

Fig. 8 : Magnetic flux density as function of Z.

Fig. 9 : Field direction as function of Z.

Fig. 10 : Axial flux density as function of Z.

Fig. 11 : Radial flux density as function of Z.

Fig. 12 : Magnetic flux density as function of R.

Fig. 13 : Field direction as function of R.

Fig. 14 : Axial flux density as function of R.

Fig. 15 : Radial flux density as function of R.

Fig. 16 : Magnetic flux density and field direction as functions of T_0 R_0 = 310.

Fig. 17 : Magnetic flux density and field direction as functions of T_0 R_0 = 410.

Fig. 18 : Magnetic flux density and field direction as functions of T_0 R_0 = 560.

Fig. 19 : Axial flux density and radial flux density as functions of T_0 R_0 = 310.

Fig. 20 : Axial flux density and radial flux density as functions of T_0 R_0 = 410.

Fig. 21 : Axial flux density and radial flux density as functions of T_0 R_0 = 560.

Fig. 22 : Stray field in the beam window.

Fig. 23 : Power consumption.

Fig. 24 : X-ray photograph of brazed joint of coil conductor.

Fig. 25 : Electrical circuit diagram.

Fig. 26 : Cooling water flow as a function of pressure difference.

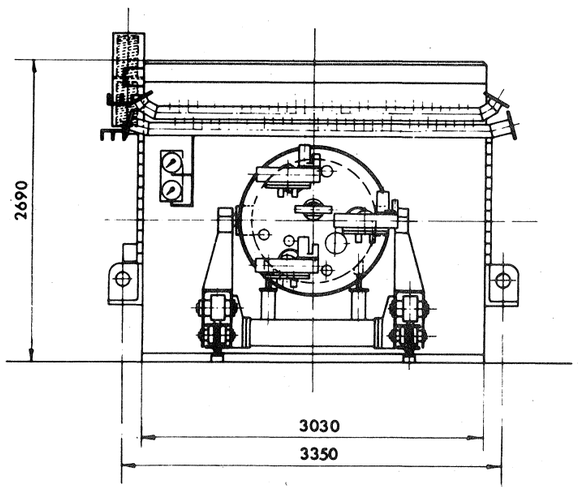

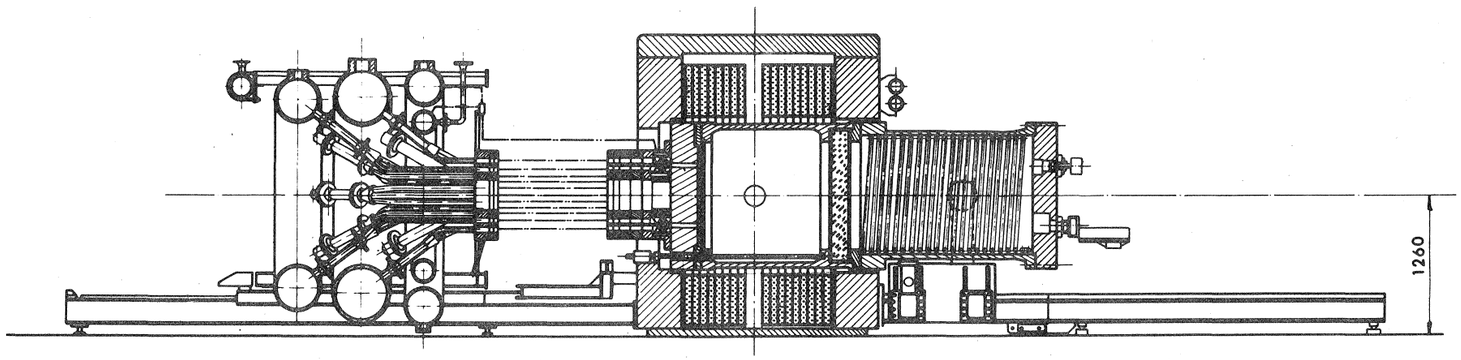

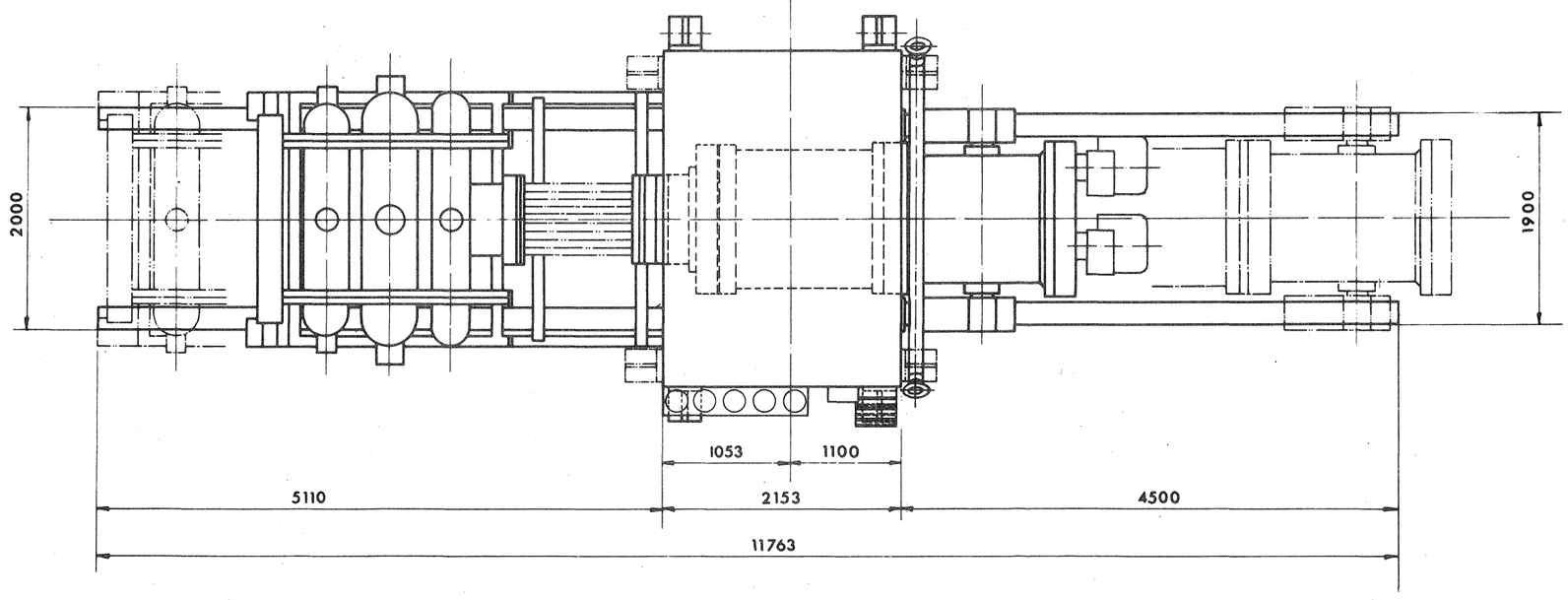

CERN – NPA 201·243·1

THE 1,1 m^3 CHAMBER
ASSEMBLED IN THE MAGNET

Fig. 1

SIS/R/16433

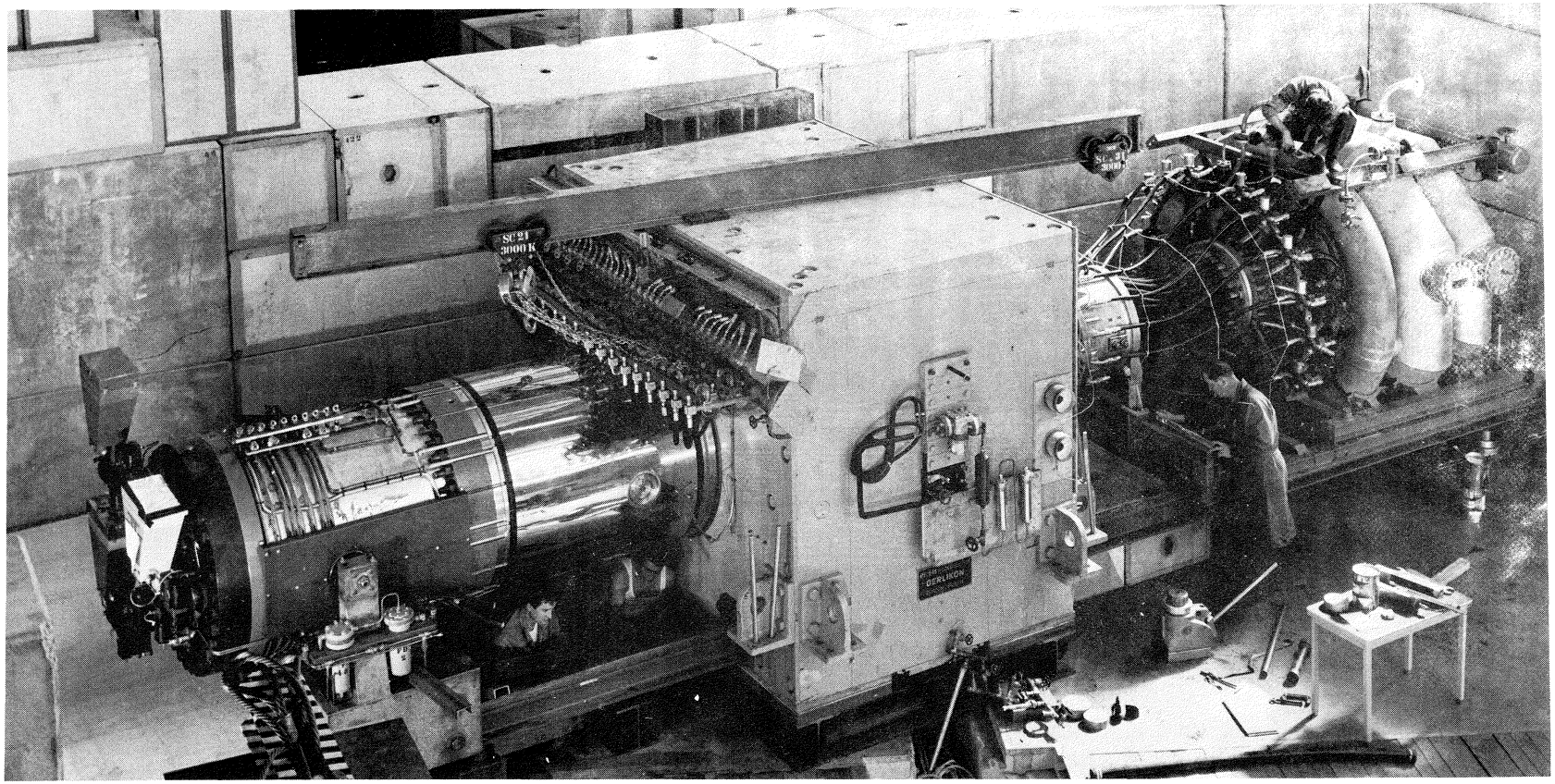

PHOTOGRAPHIC VIEW OF THE 1,1 m^3 CHAMBER

Fig. 2

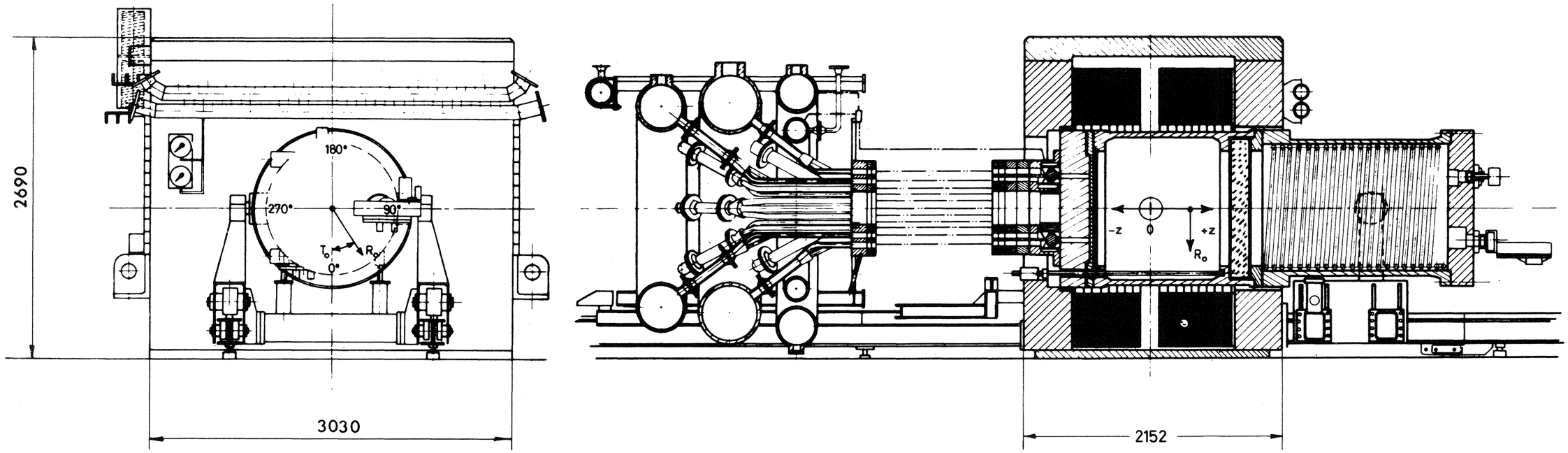

REFERENCE FRAME

FIG.3

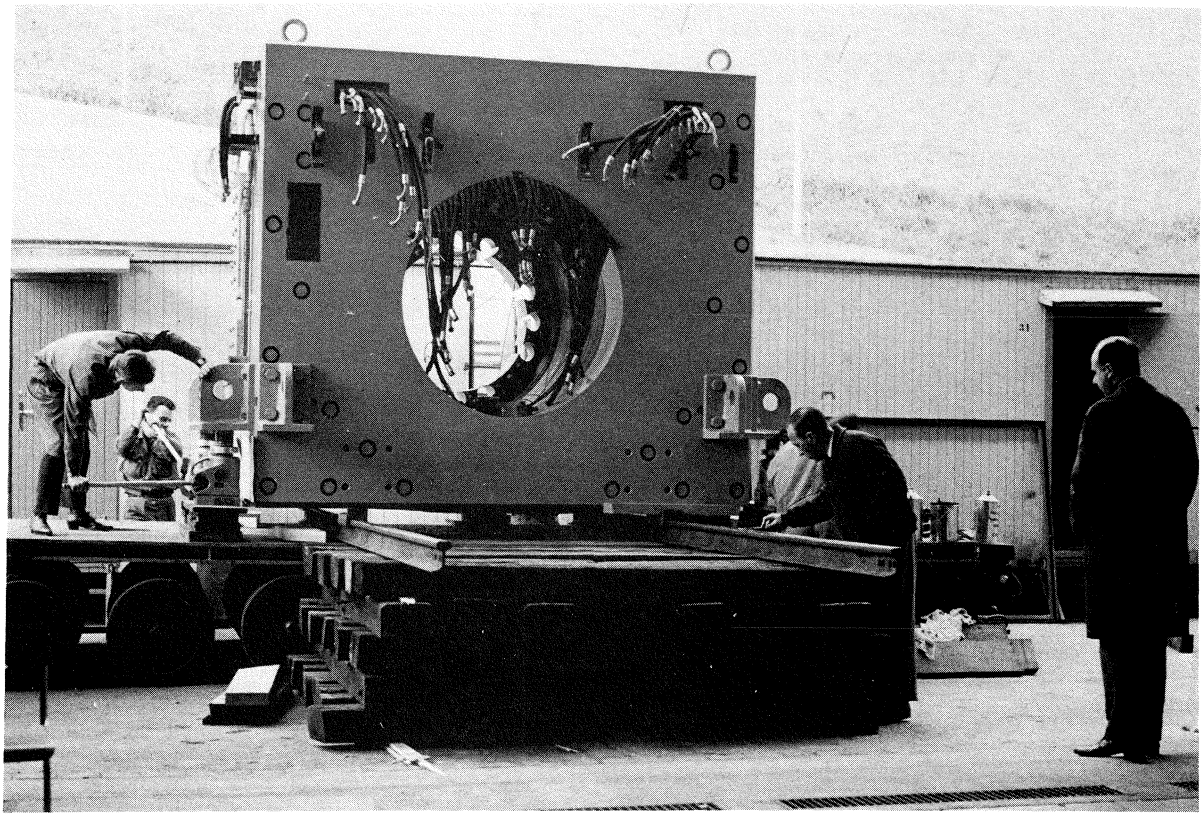

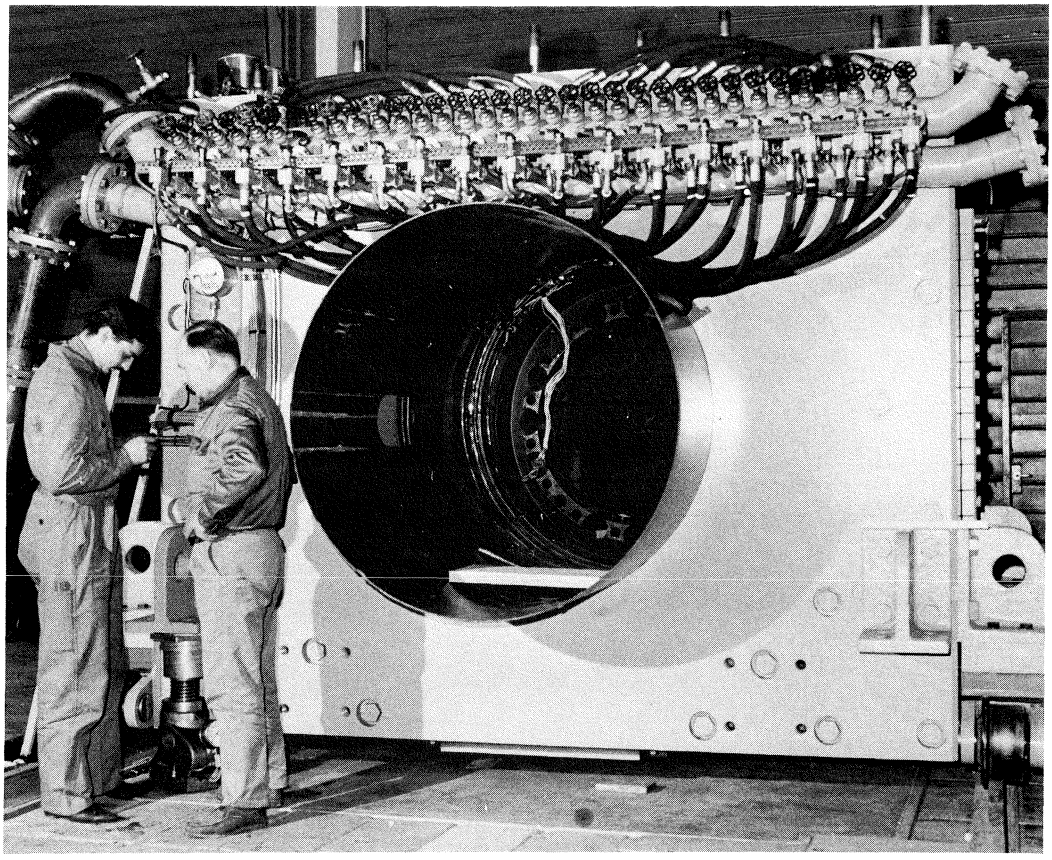

PHOTOGRAPHIC VIEWS OF THE MAGNET

Fig. 4

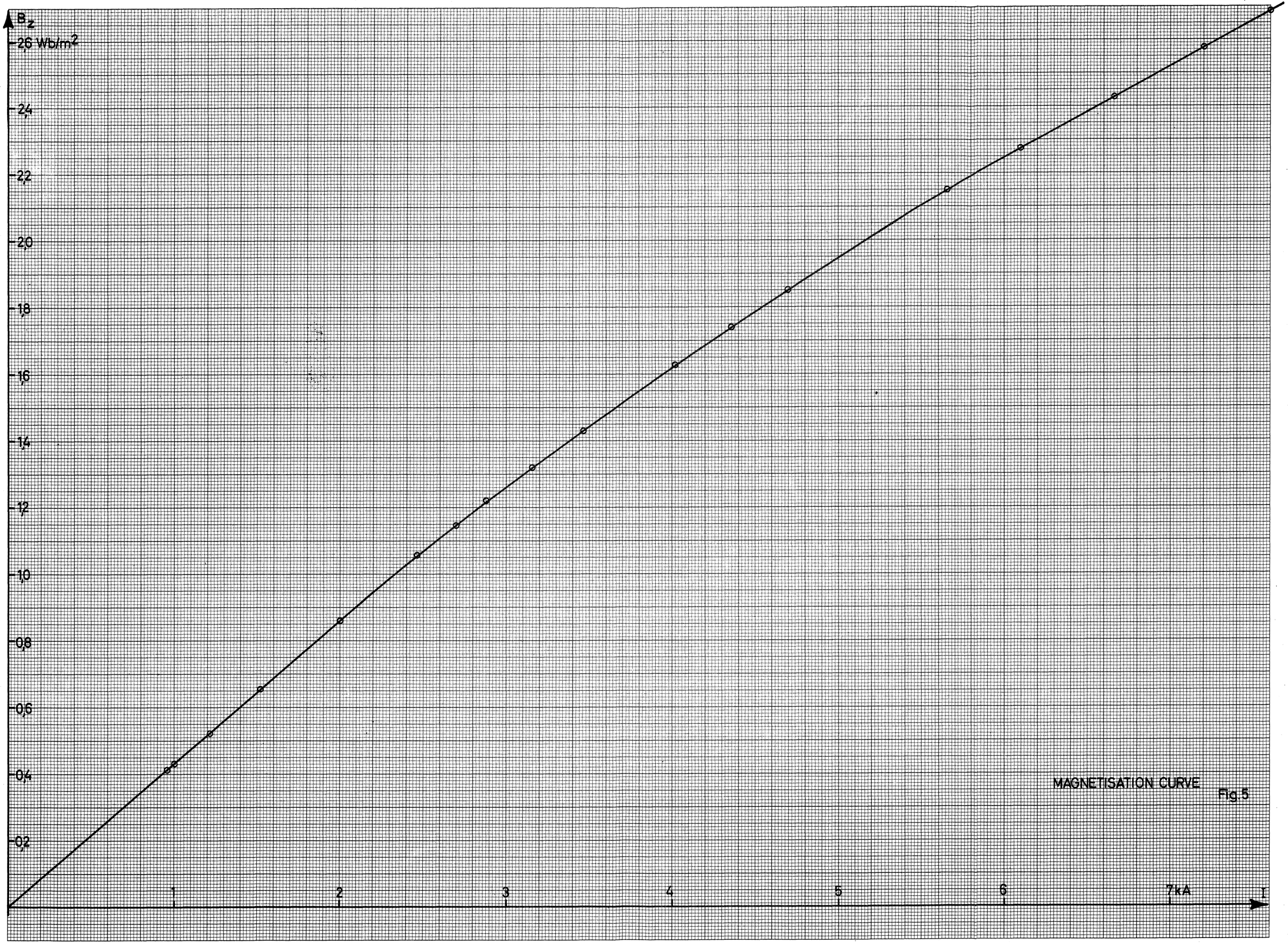

MAGNETISATION CURVE Fig. 5

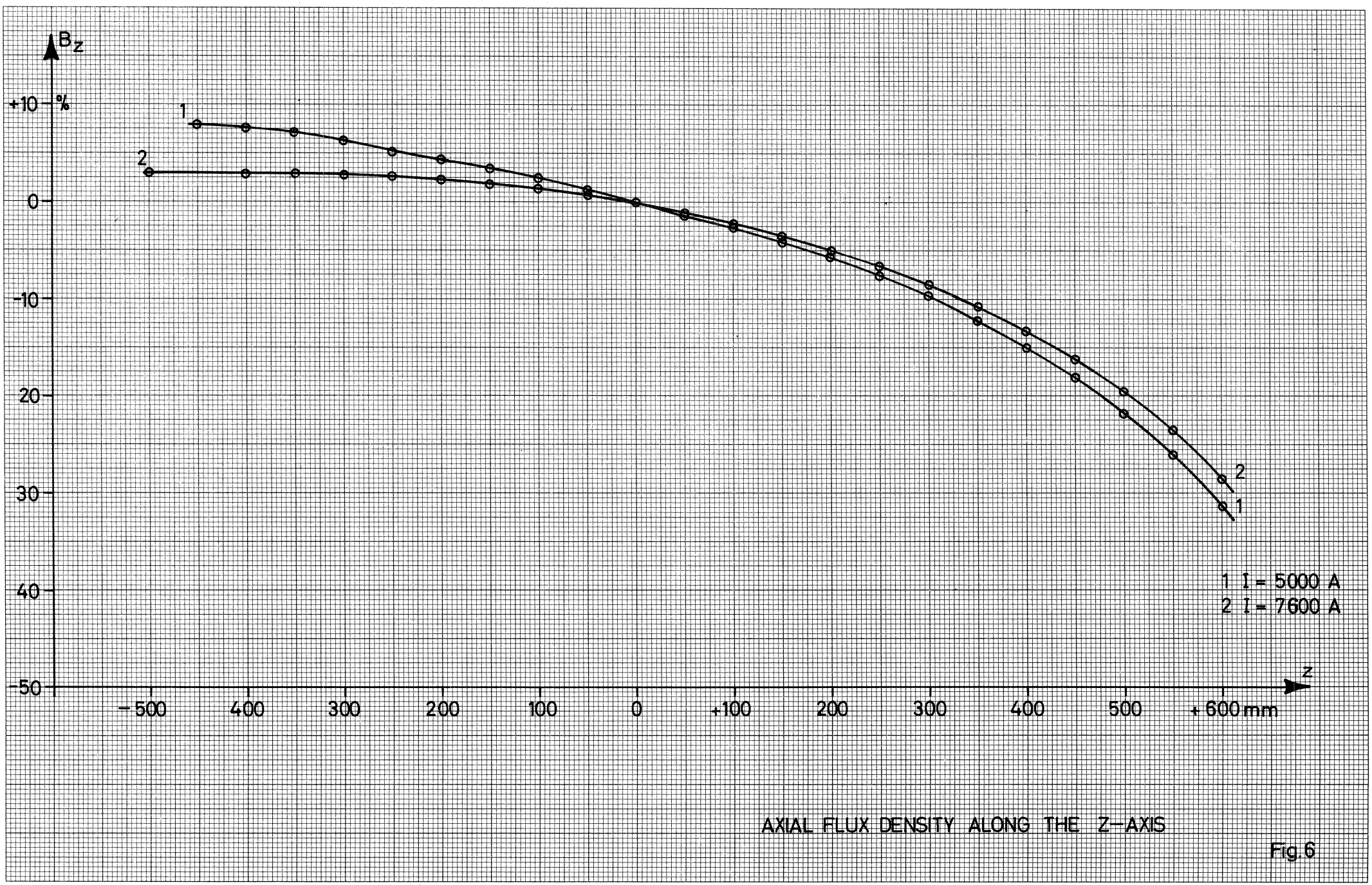

AXIAL FLUX DENSITY ALONG THE Z-AXIS

Fig. 6

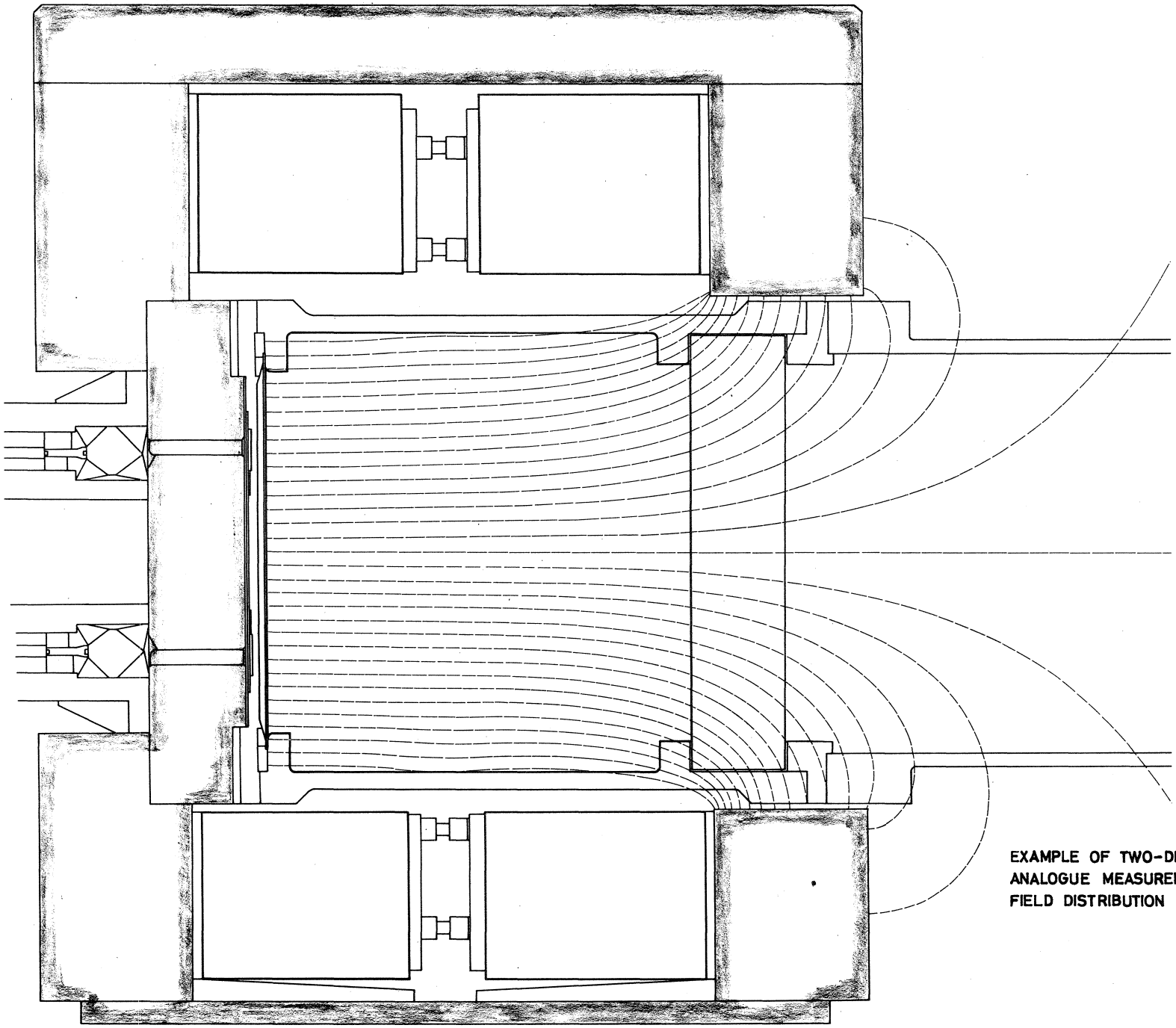

EXAMPLE OF TWO-DIMENSIONAL ANALOGUE MEASUREMENT OF FIELD DISTRIBUTION

Fig. 7

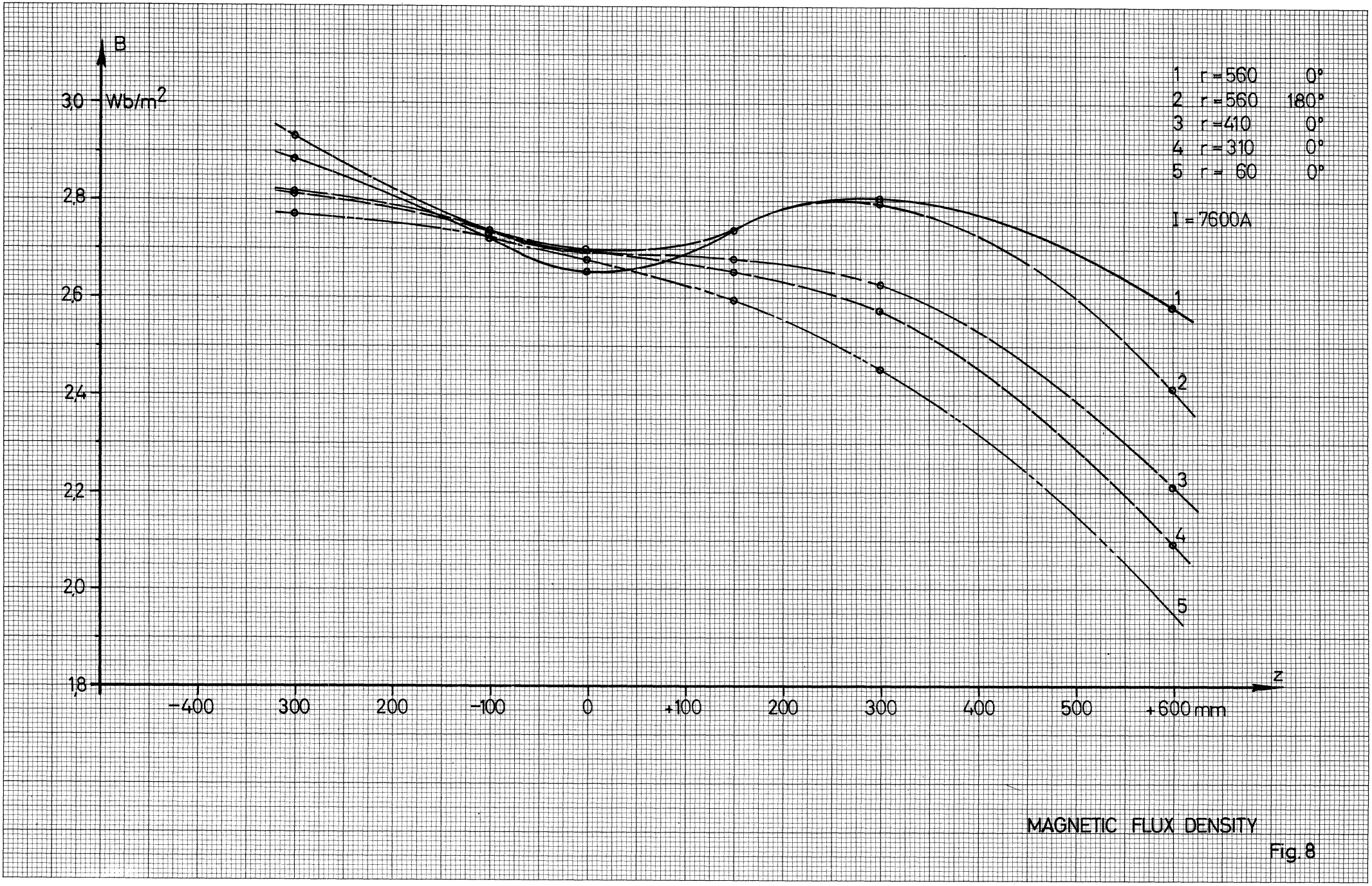

MAGNETIC FLUX DENSITY

Fig. 8

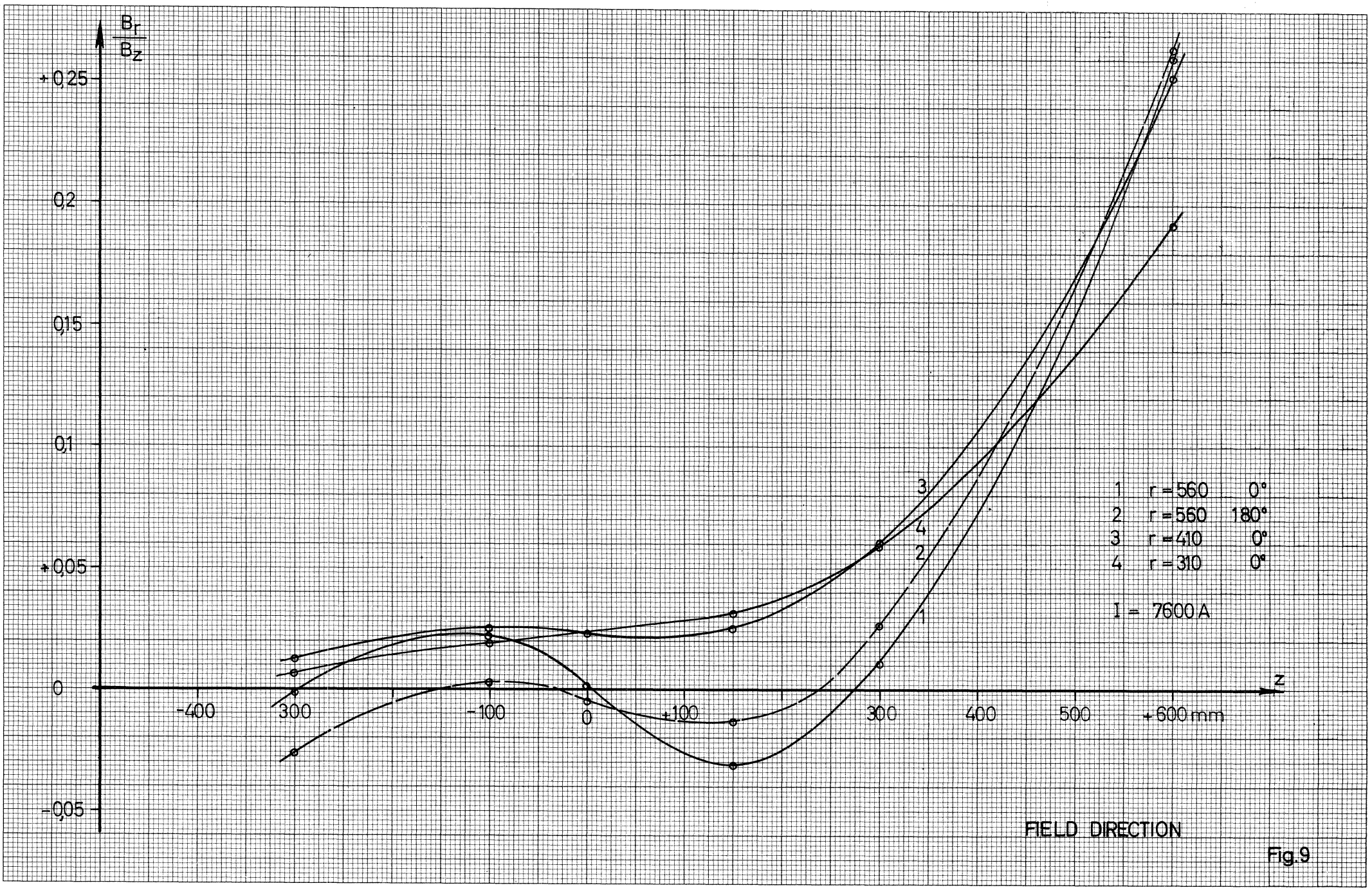
$\frac{B_r}{B_z}$
+0,25
0,2
0,15
0,1
+0,05
0
-0,005
-400
300
-100
0
+100
300
400
500
+600 mm
z
1 r = 560 0°
2 r = 560 180°
3 r = 410 0°
4 r = 310 0°
I = 7600 A
FIELD DIRECTION

Fig.9

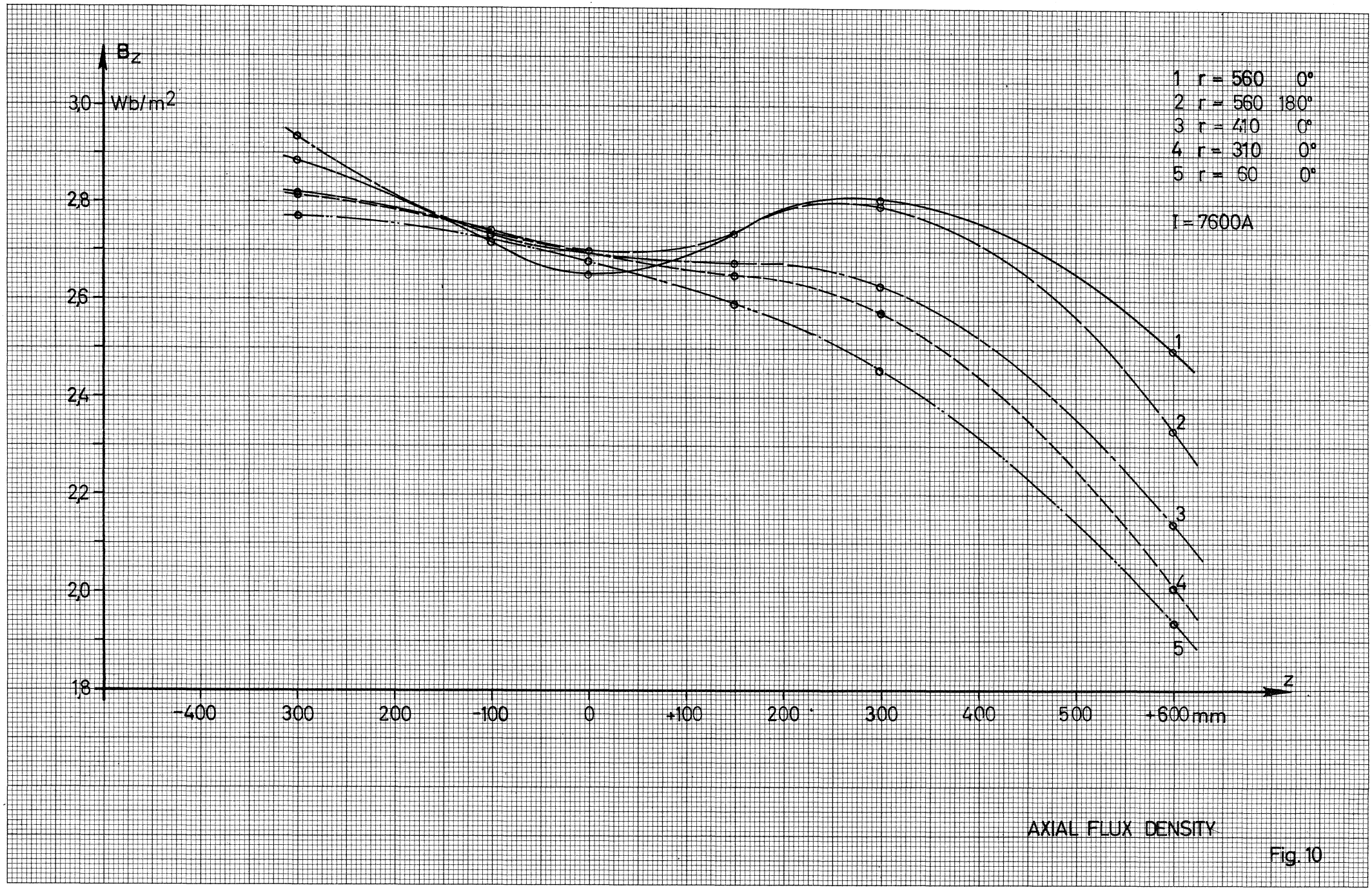

AXIAL FLUX DENSITY

Fig. 10

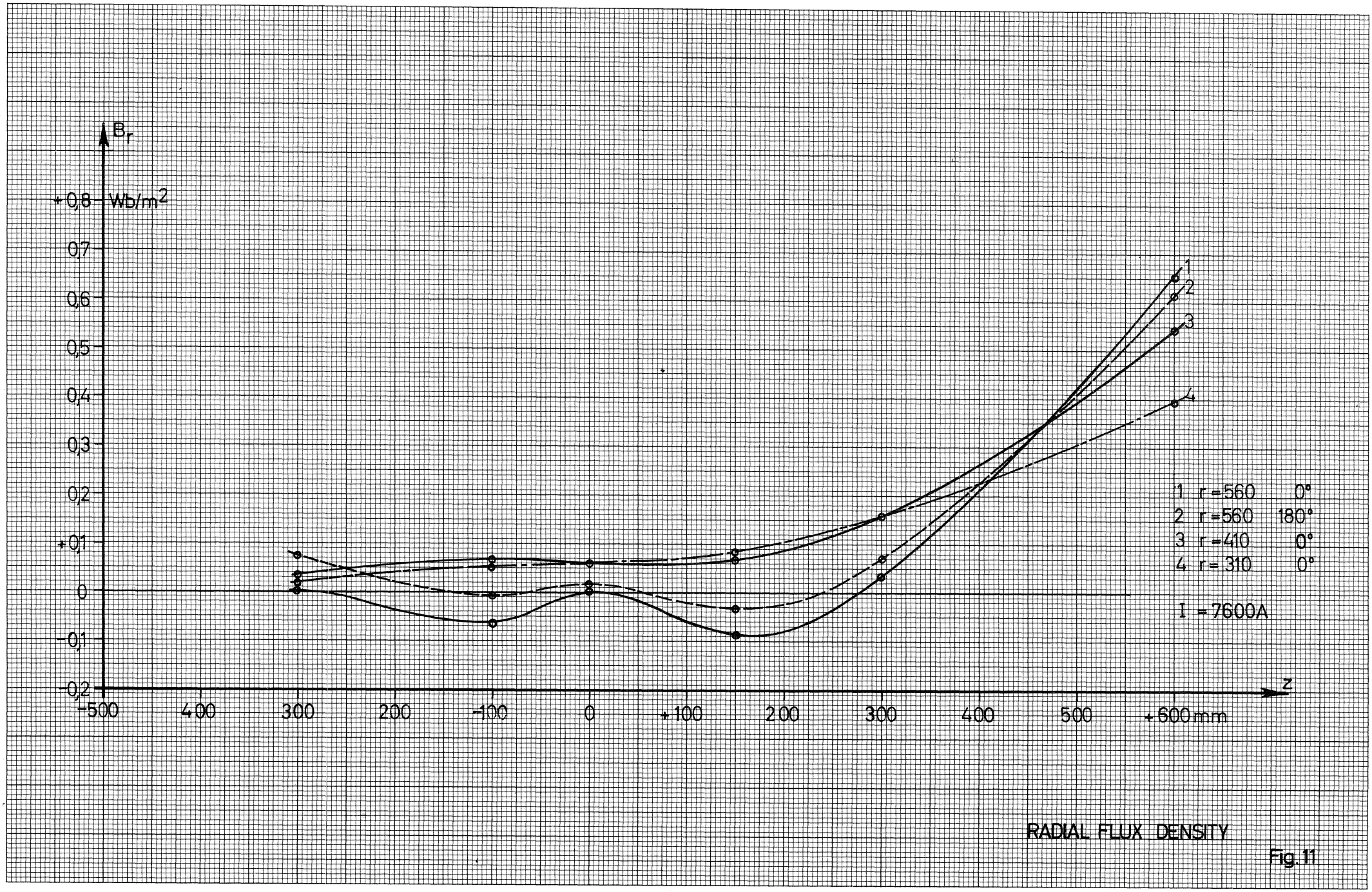

RADIAL FLUX DENSITY

Fig. 11

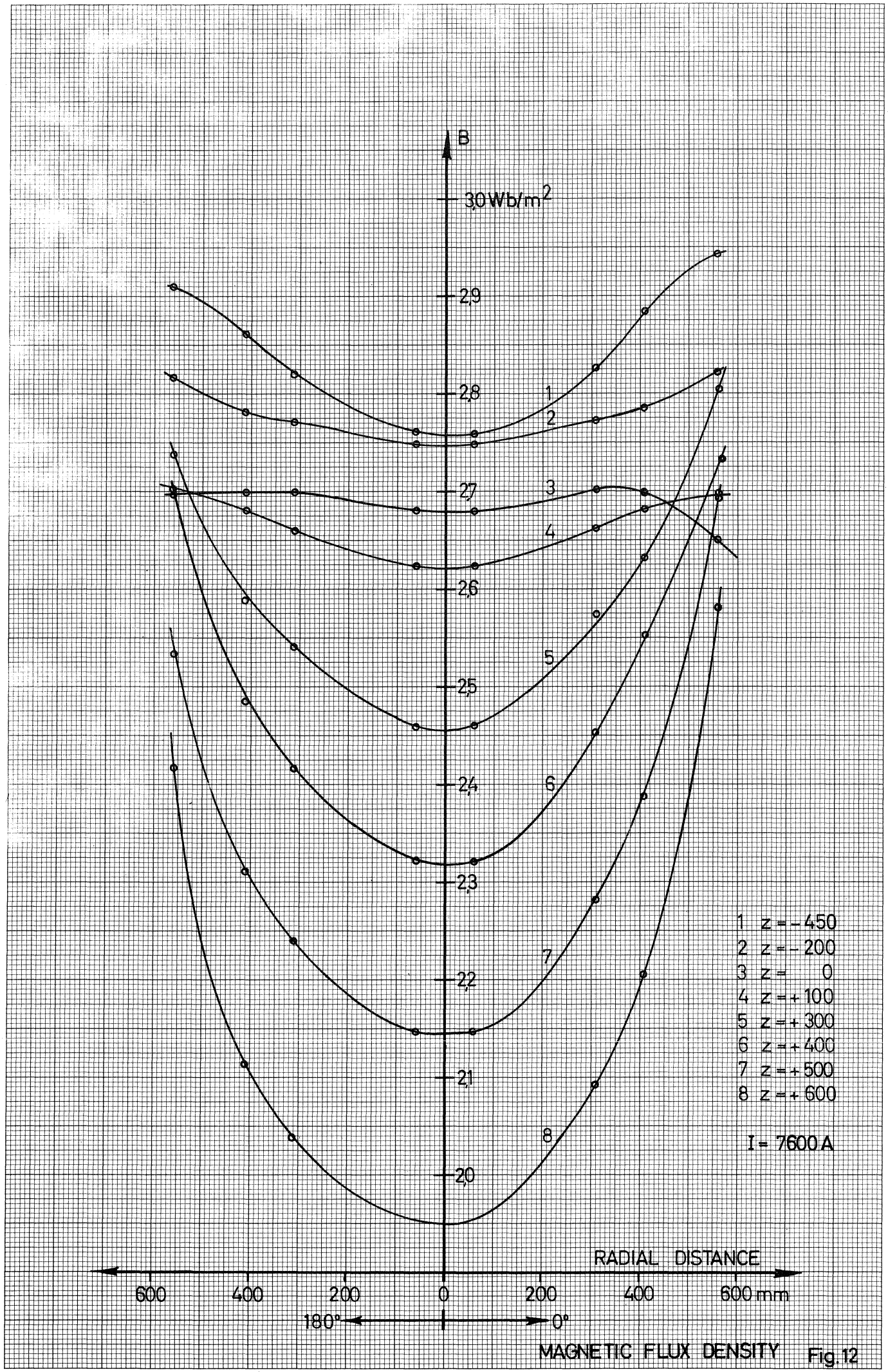

MAGNETIC FLUX DENSITY Fig. 12

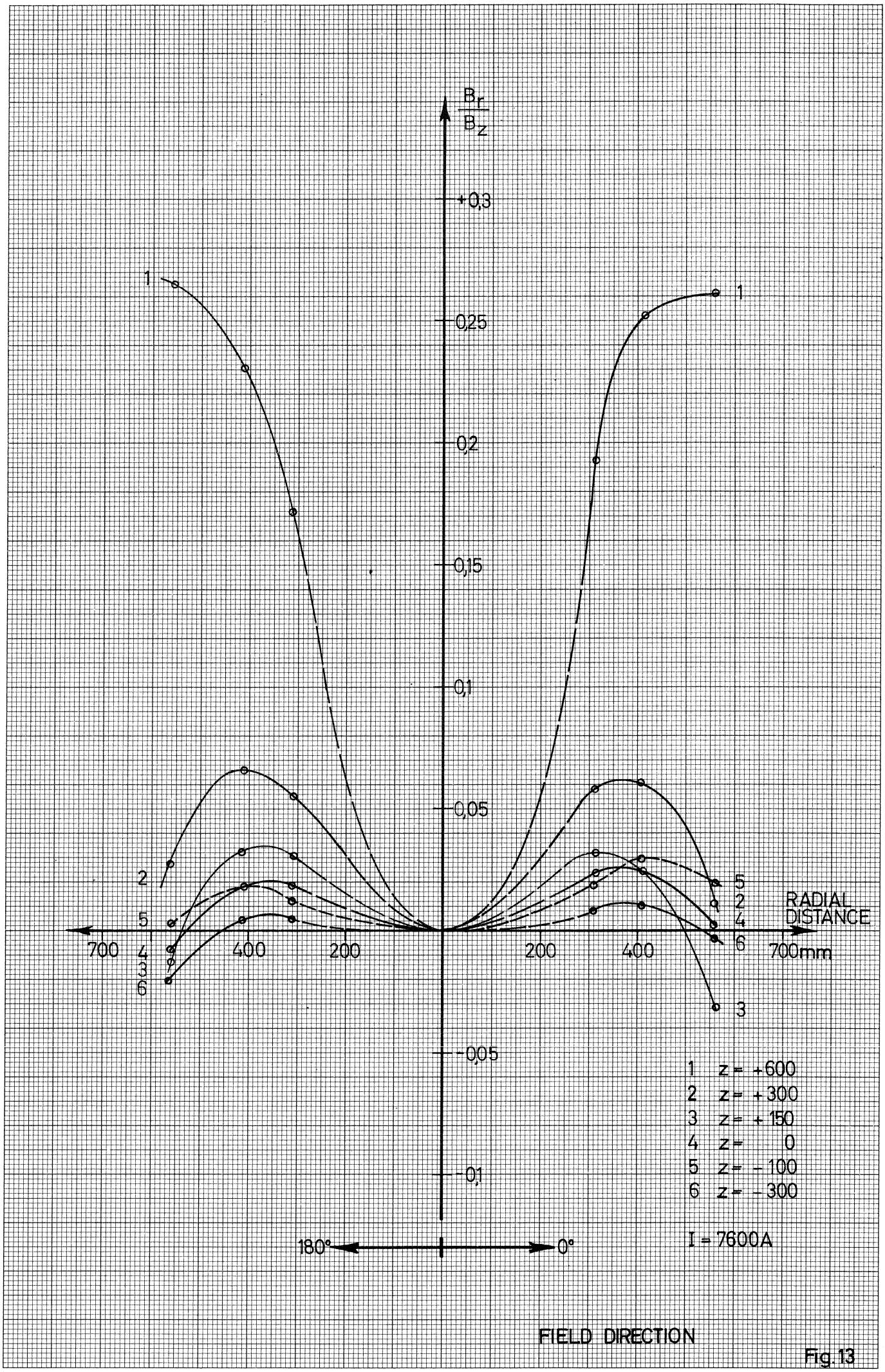
$\frac{B_r}{B_z}$
+0,3
0,25
0,2
0,15
0,1
0,05
-0,005
-0,1
700
400
200
200
400
700mm
RADIAL DISTANCE
180°
0°
FIELD DIRECTION
1 z = +600
2 z = +300
3 z = +150
4 z = 0
5 z = -100
6 z = -300
I = 7600A

Fig. 13

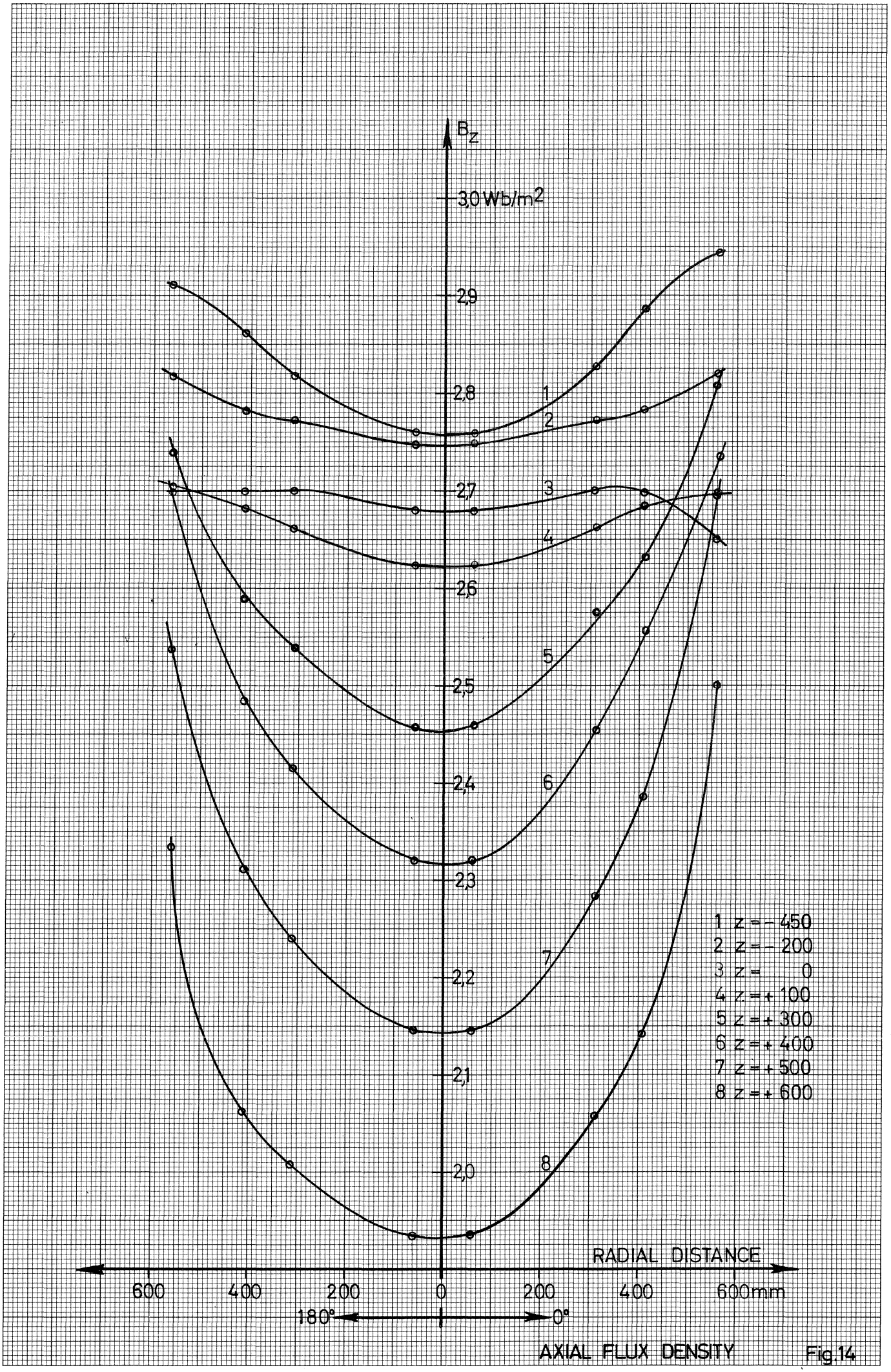

AXIAL FLUX DENSITY

Fig.14

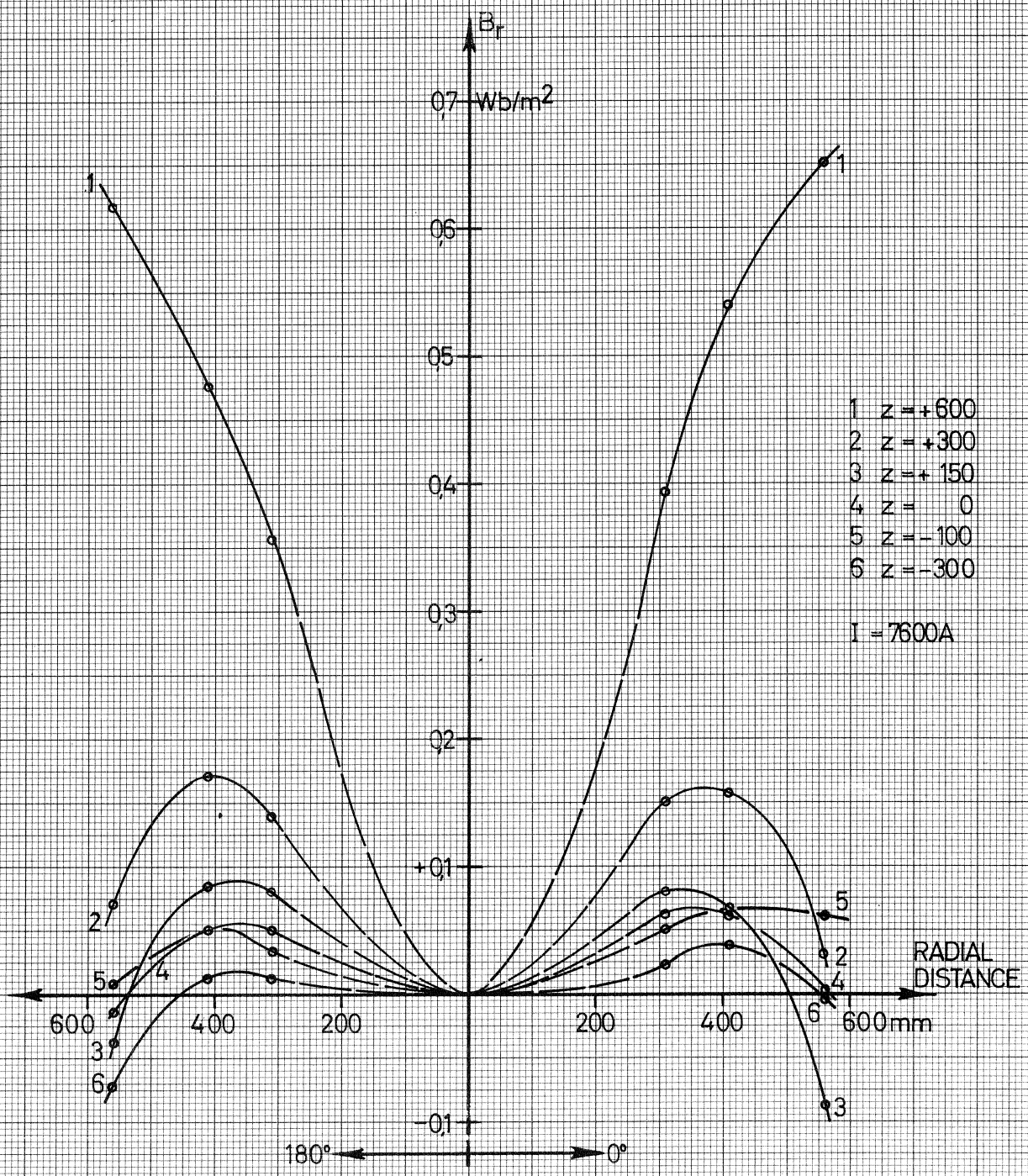

RADIAL FLUX DENSITY

Fig. 15

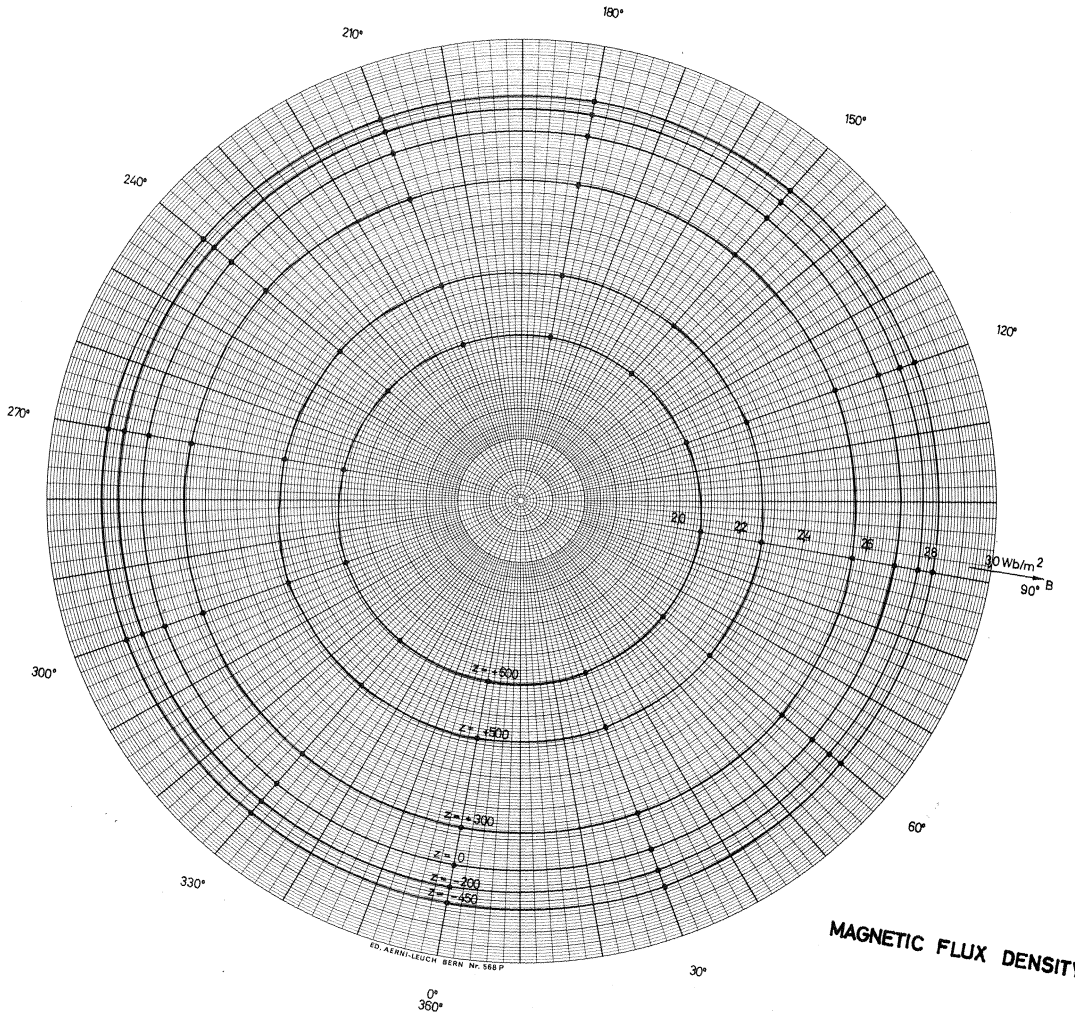

MAGNETIC FLUX DENSITY

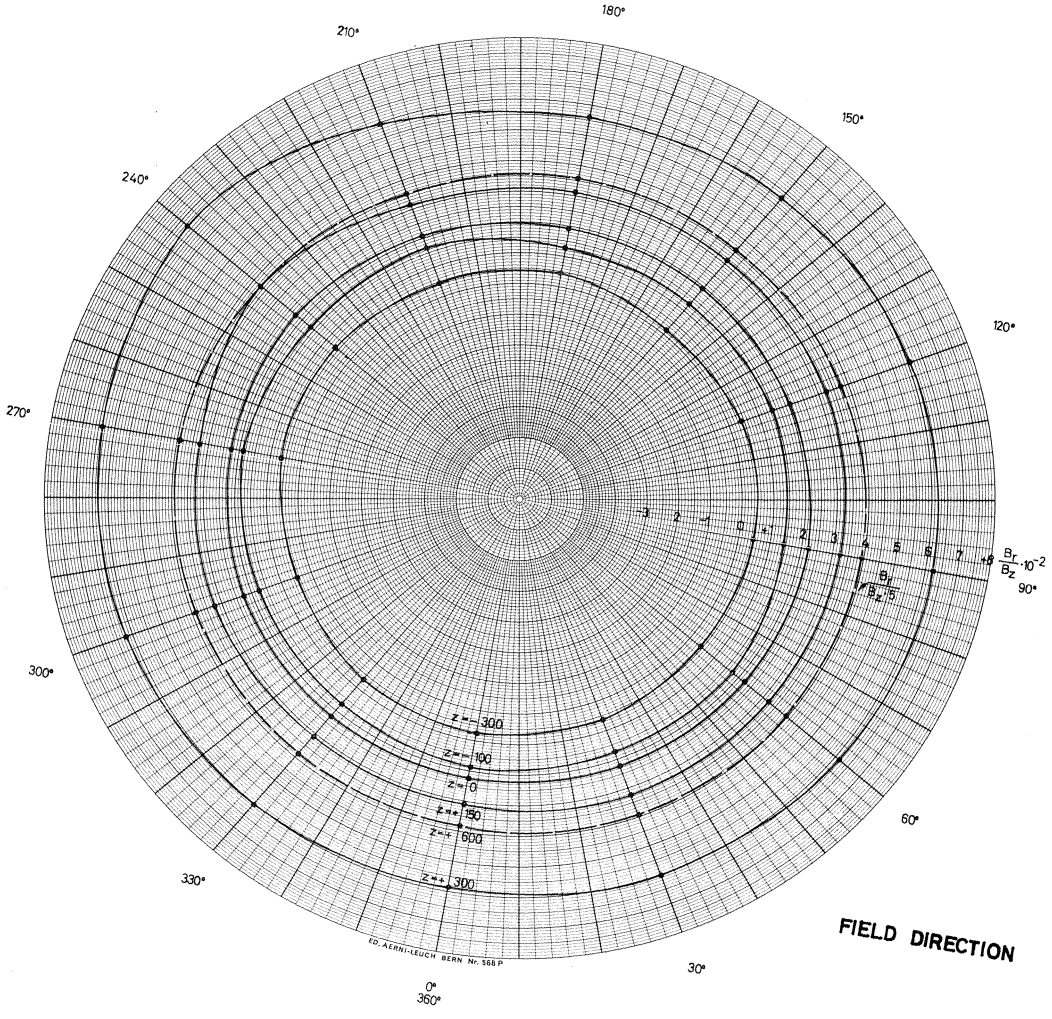

r = 310 mm
I = 7600 A

FIELD DIRECTION

Fig. 16

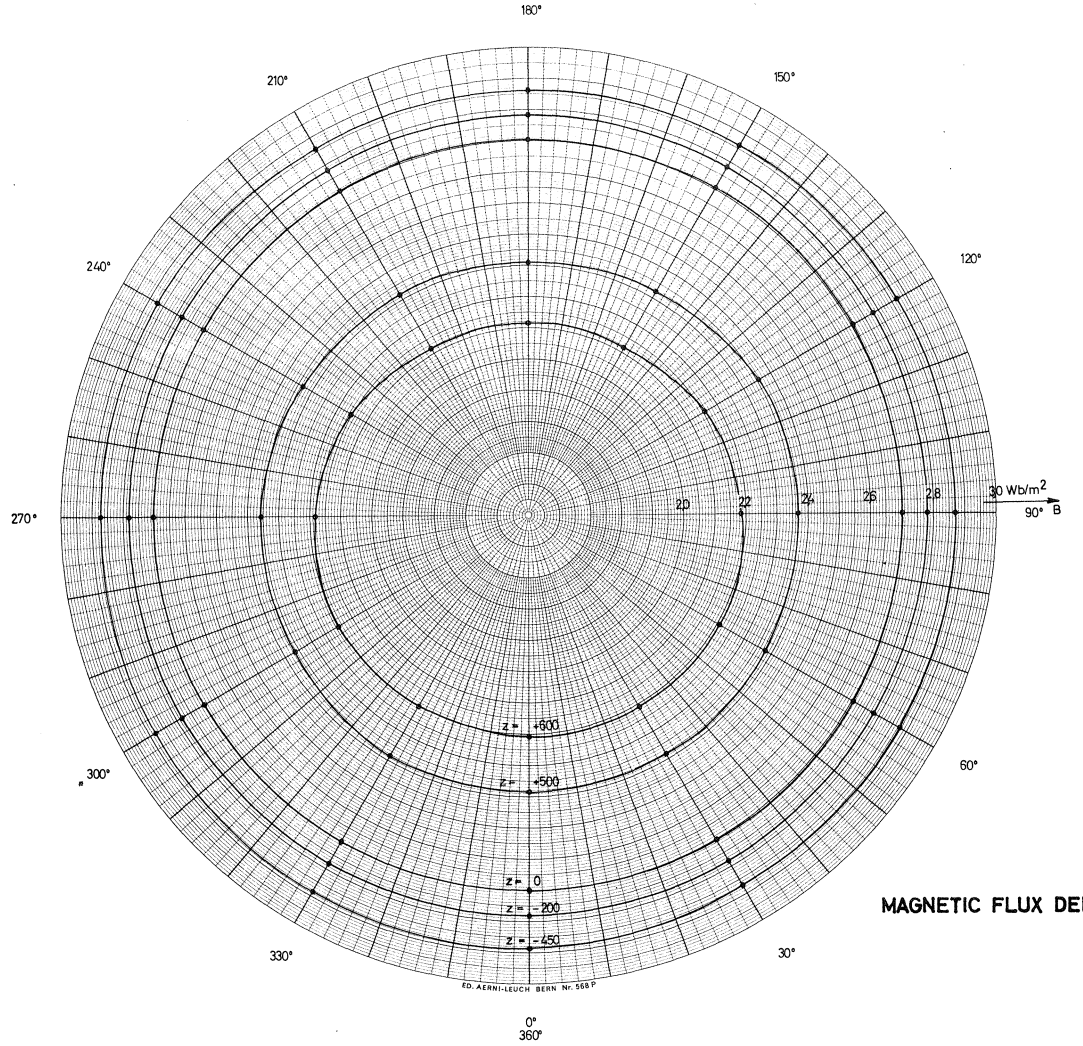

MAGNETIC FLUX DENSITY

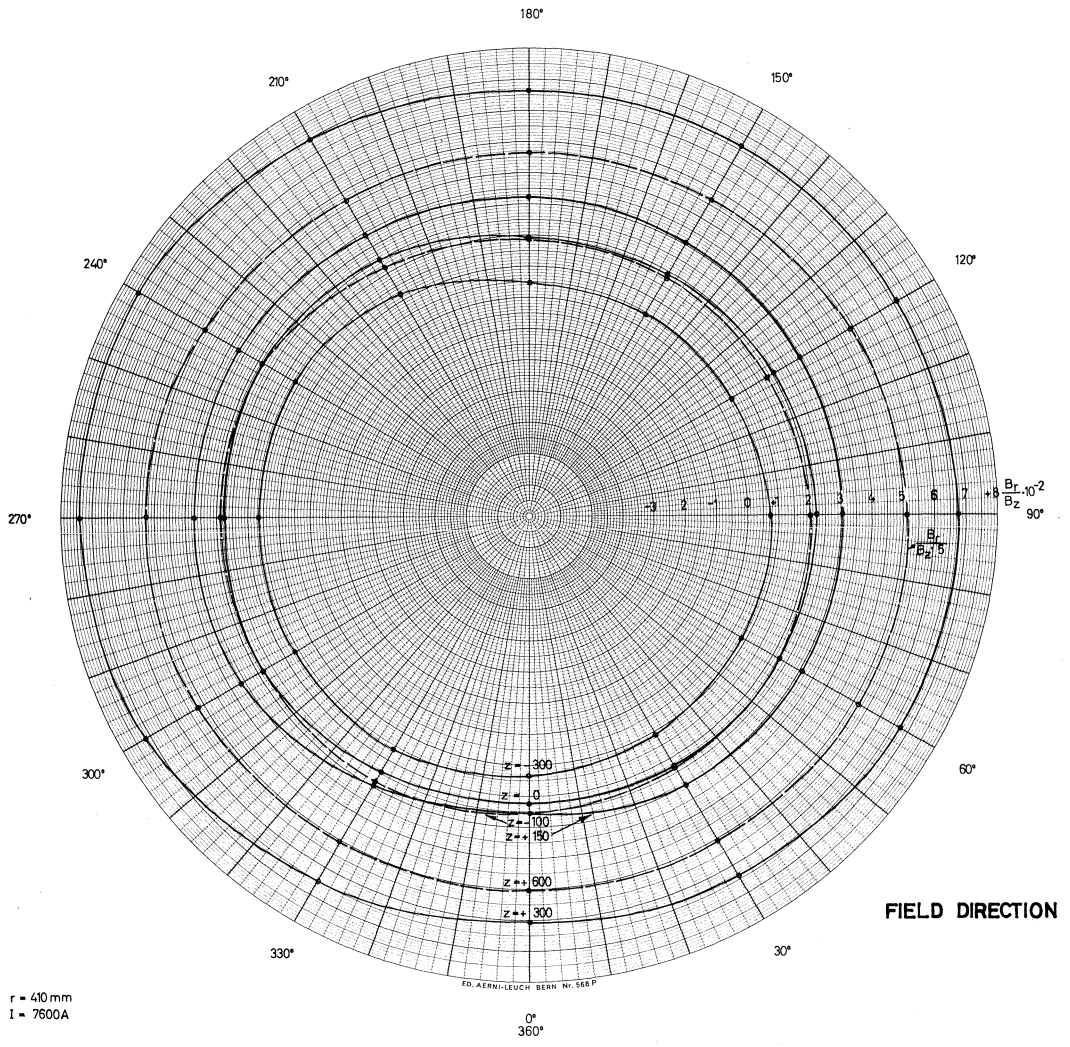

FIELD DIRECTION

r = 410 mm
I = 7600A

Fig.17

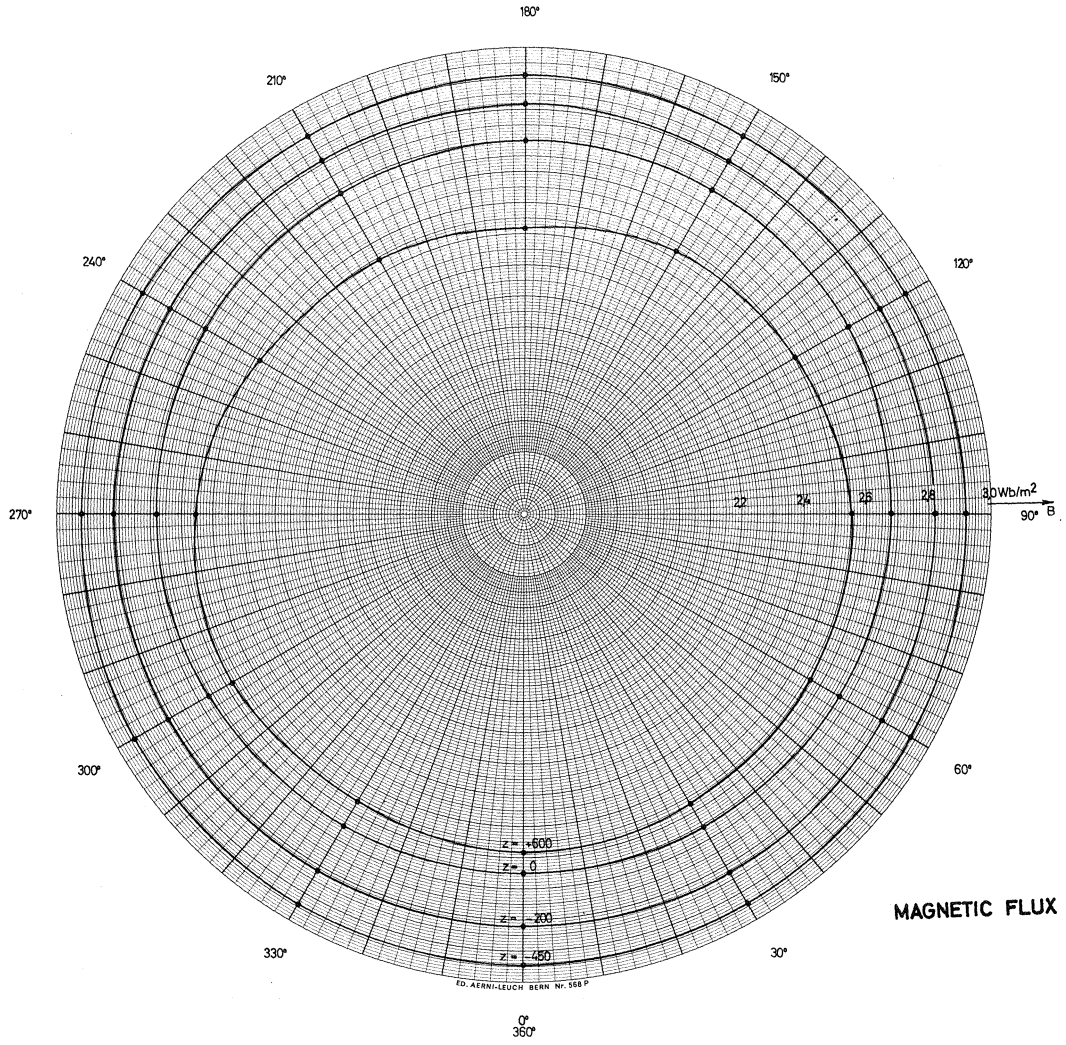

MAGNETIC FLUX DENSITY

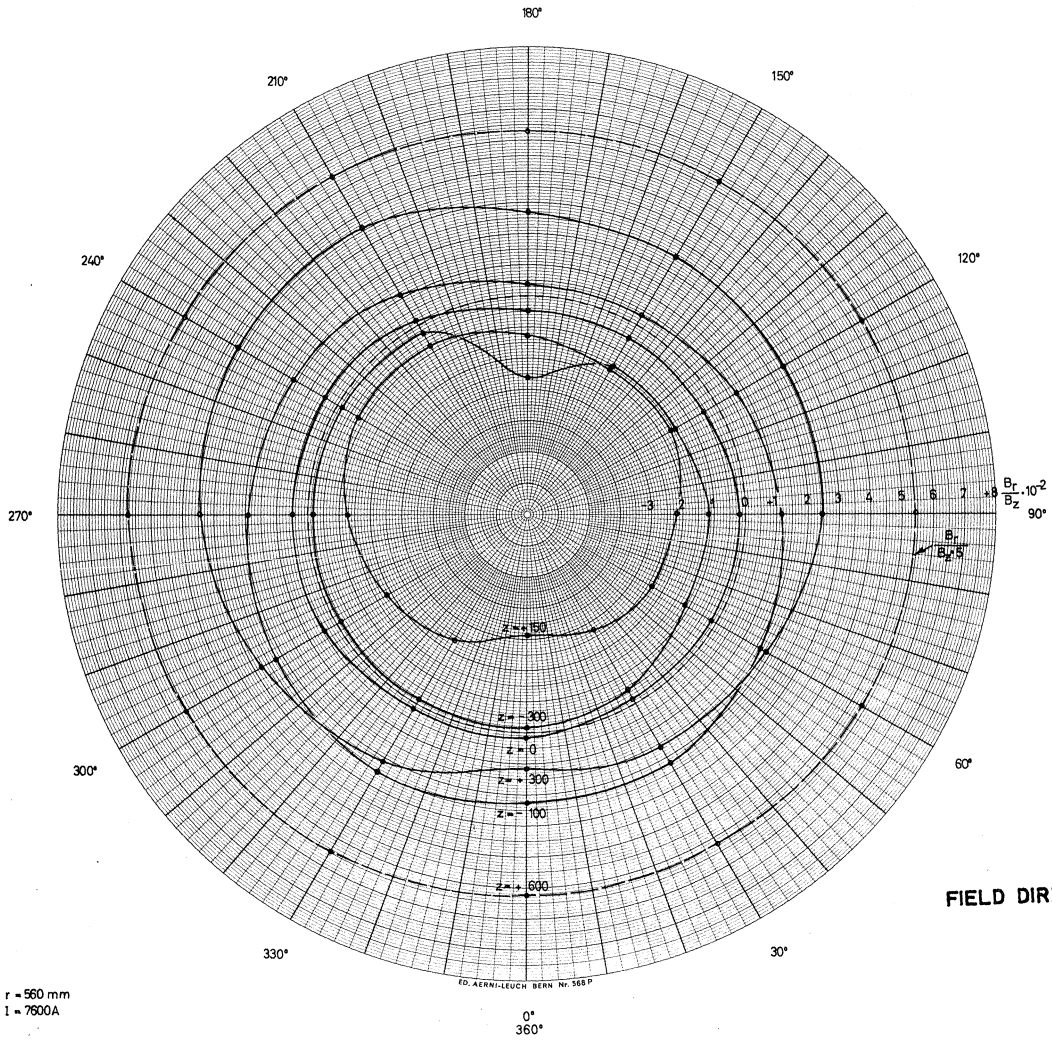

FIELD DIRECTION

r = 560 mm
I = 7600A

Fig.18

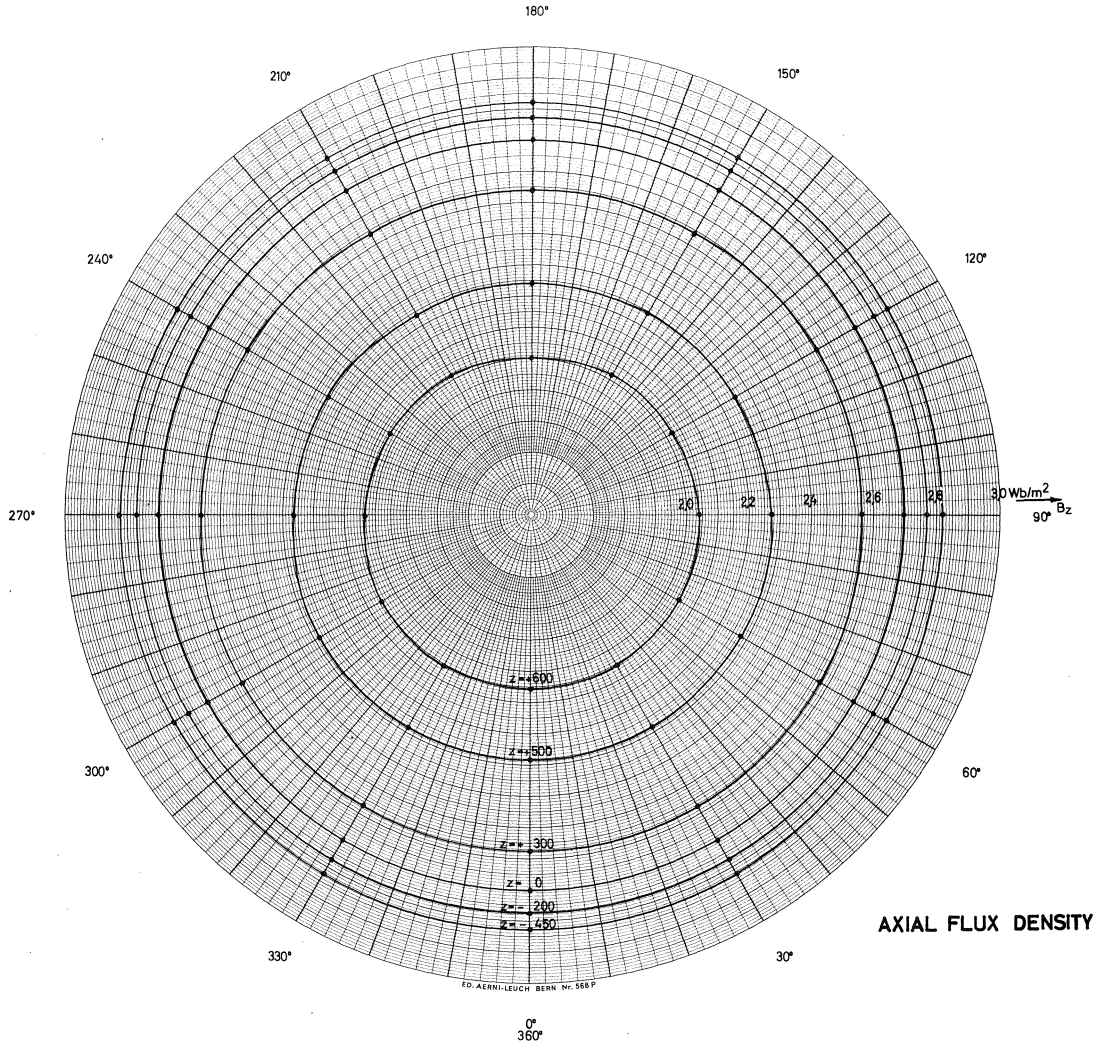

AXIAL FLUX DENSITY

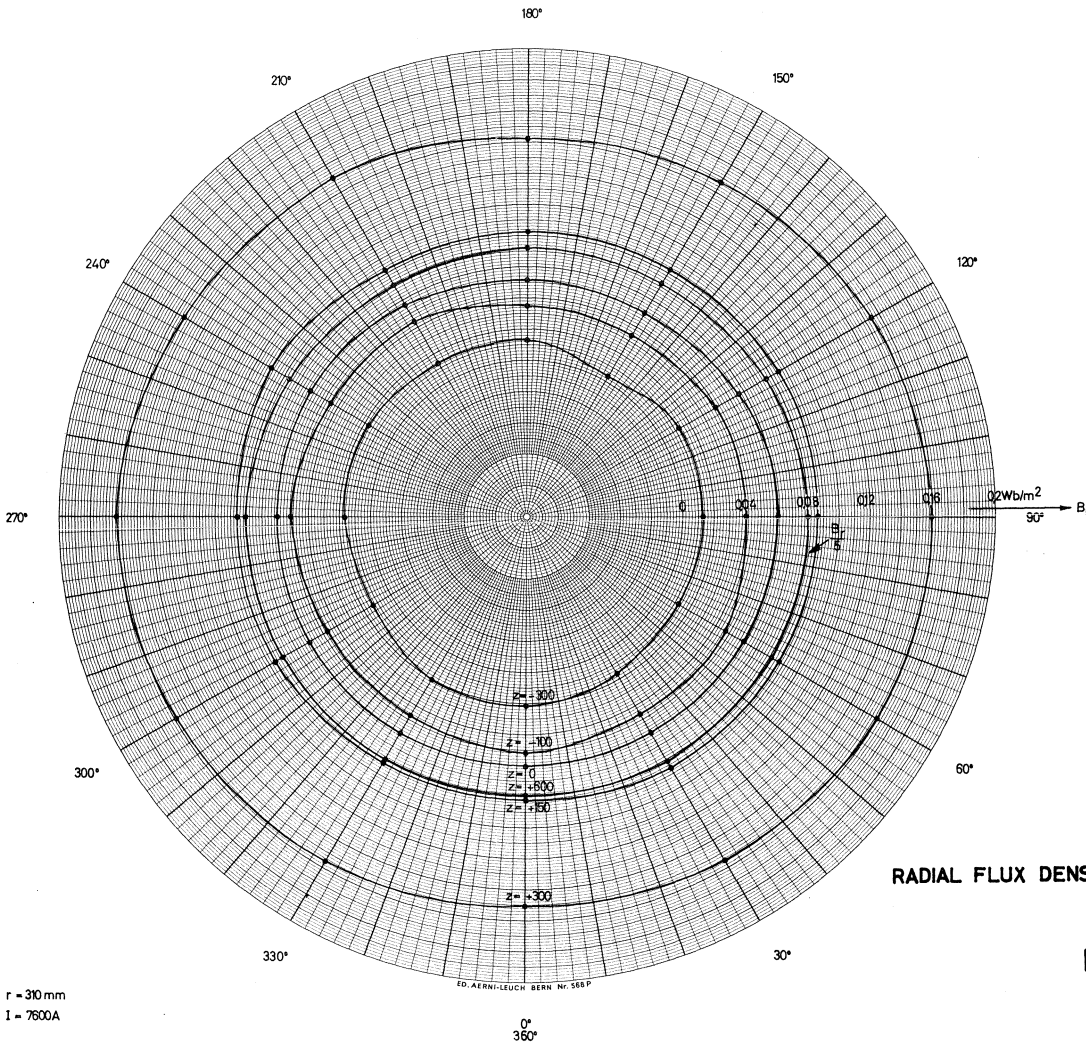

RADIAL FLUX DENSITY

Fig. 19

r = 310 mm
I = 7600 A

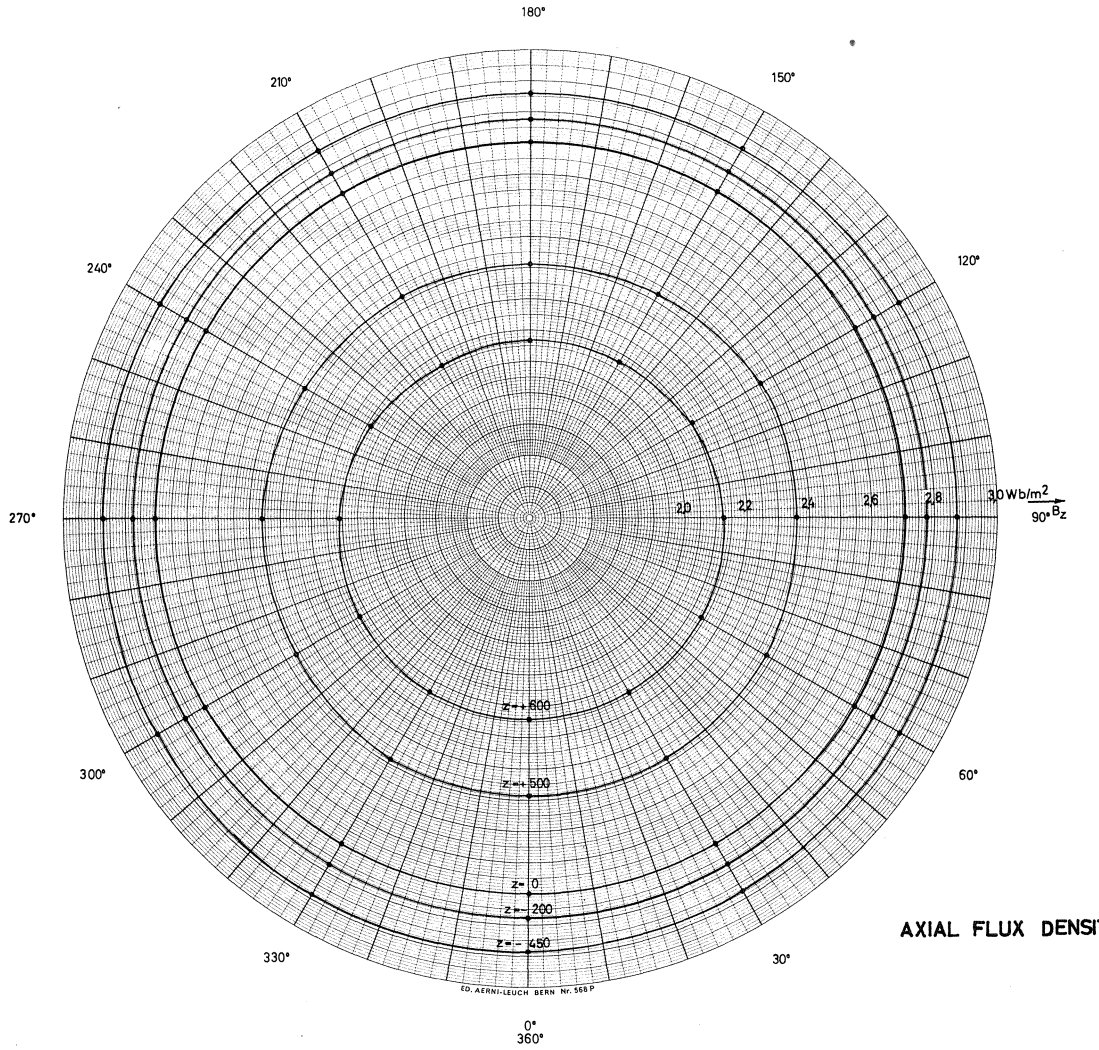

AXIAL FLUX DENSITY

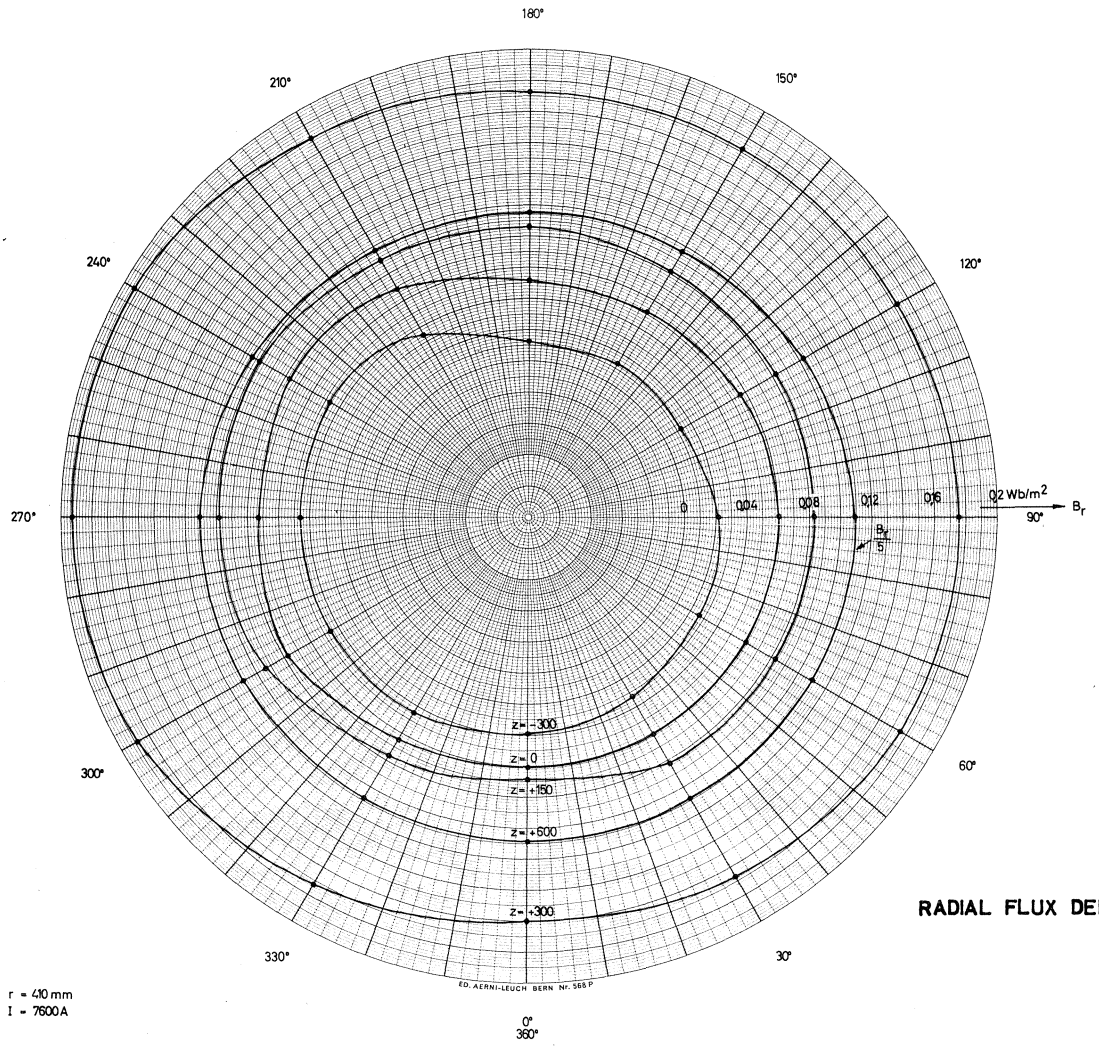

RADIAL FLUX DENSITY

r = 410 mm
I = 7600 A

Fig. 20

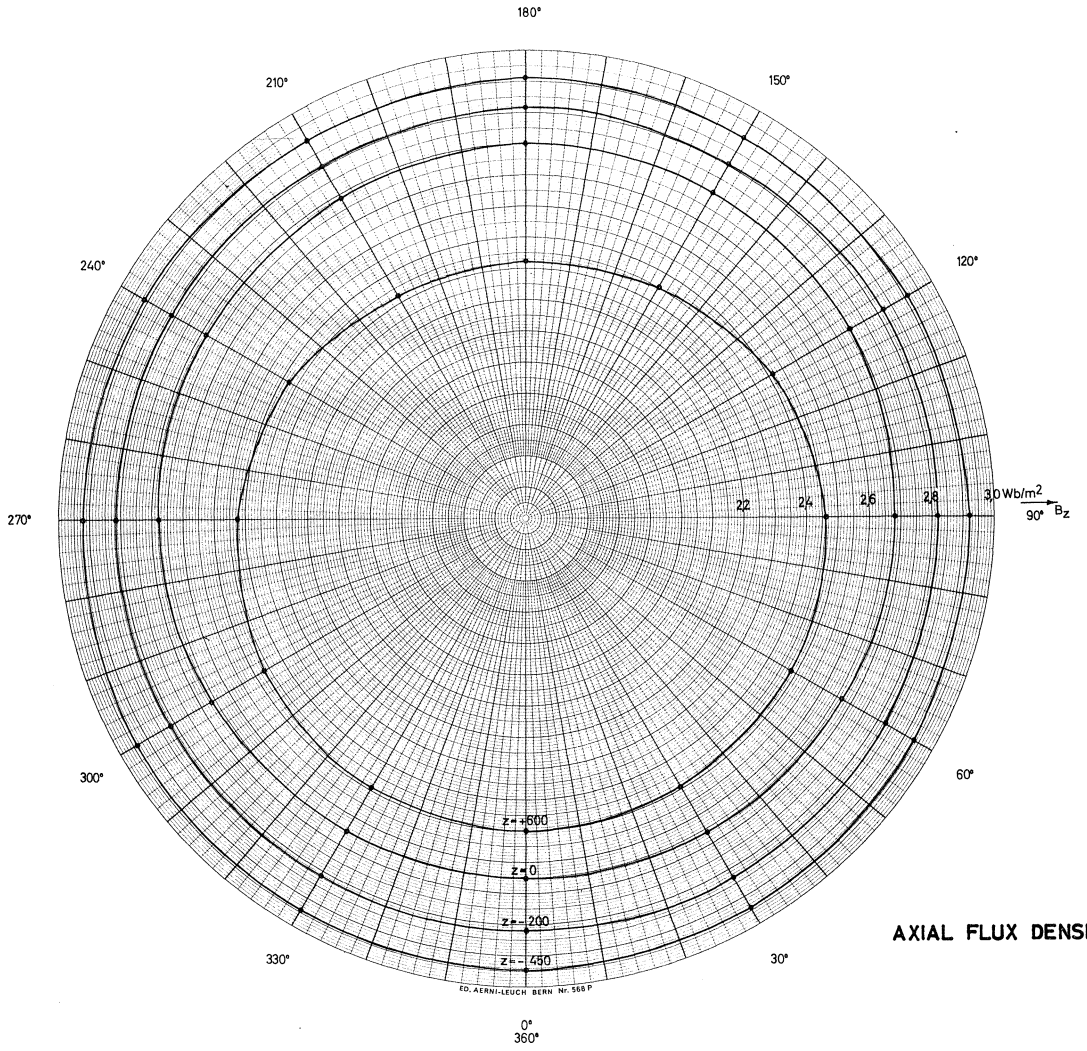

AXIAL FLUX DENSITY

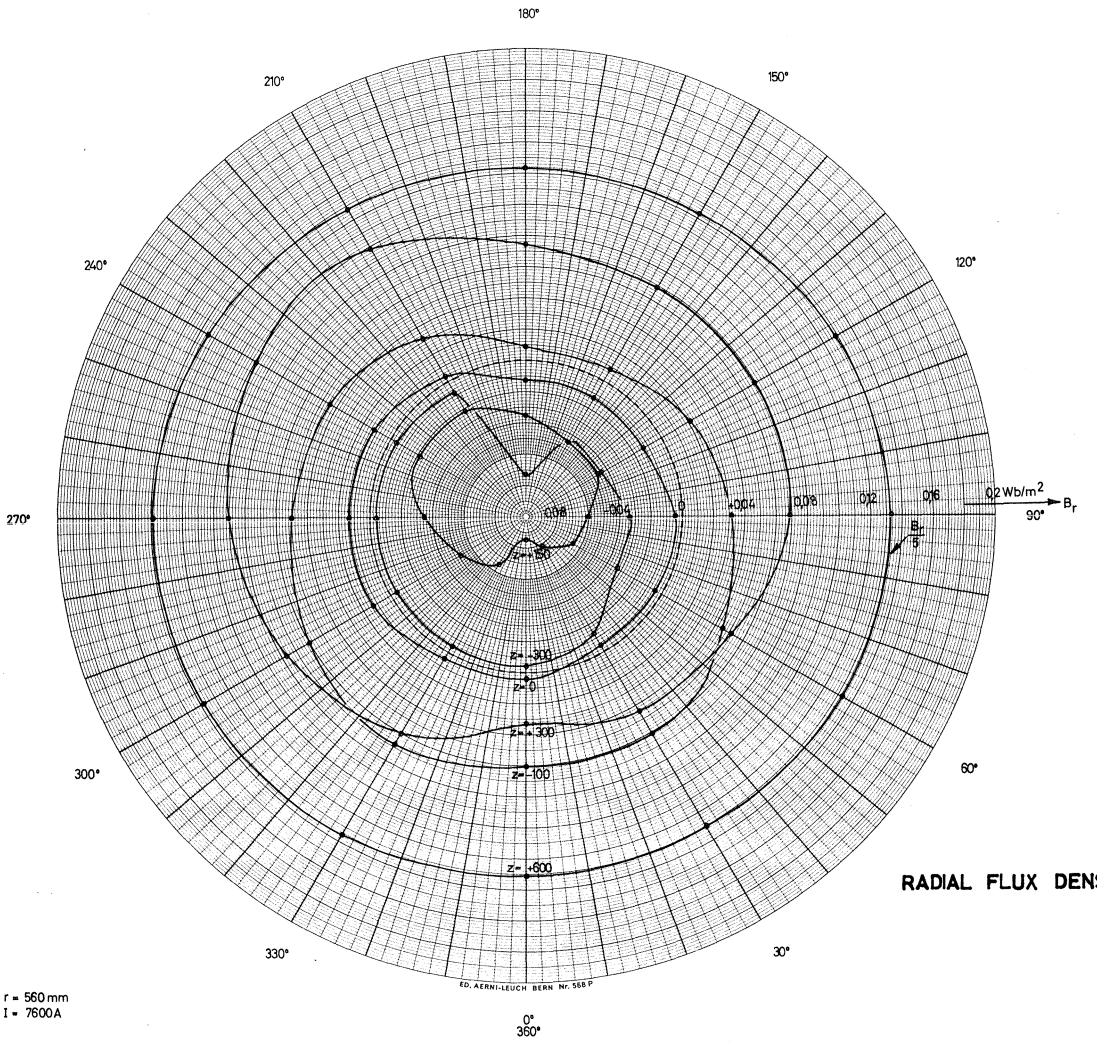

RADIAL FLUX DENSITY

Fig. 21

r = 560 mm
I = 7600 A

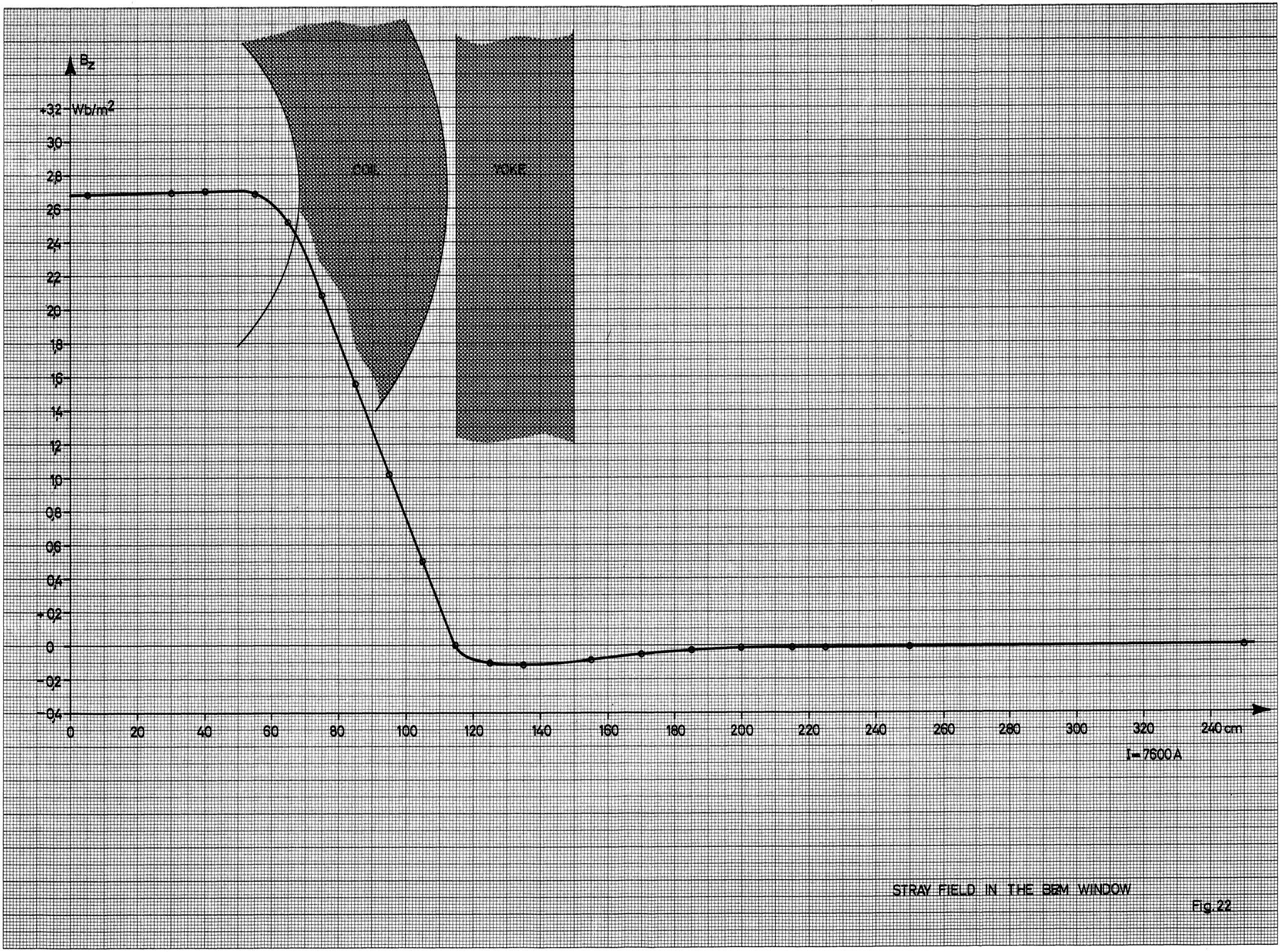

STRAY FIELD IN THE BEAM WINDOW

Fig. 22

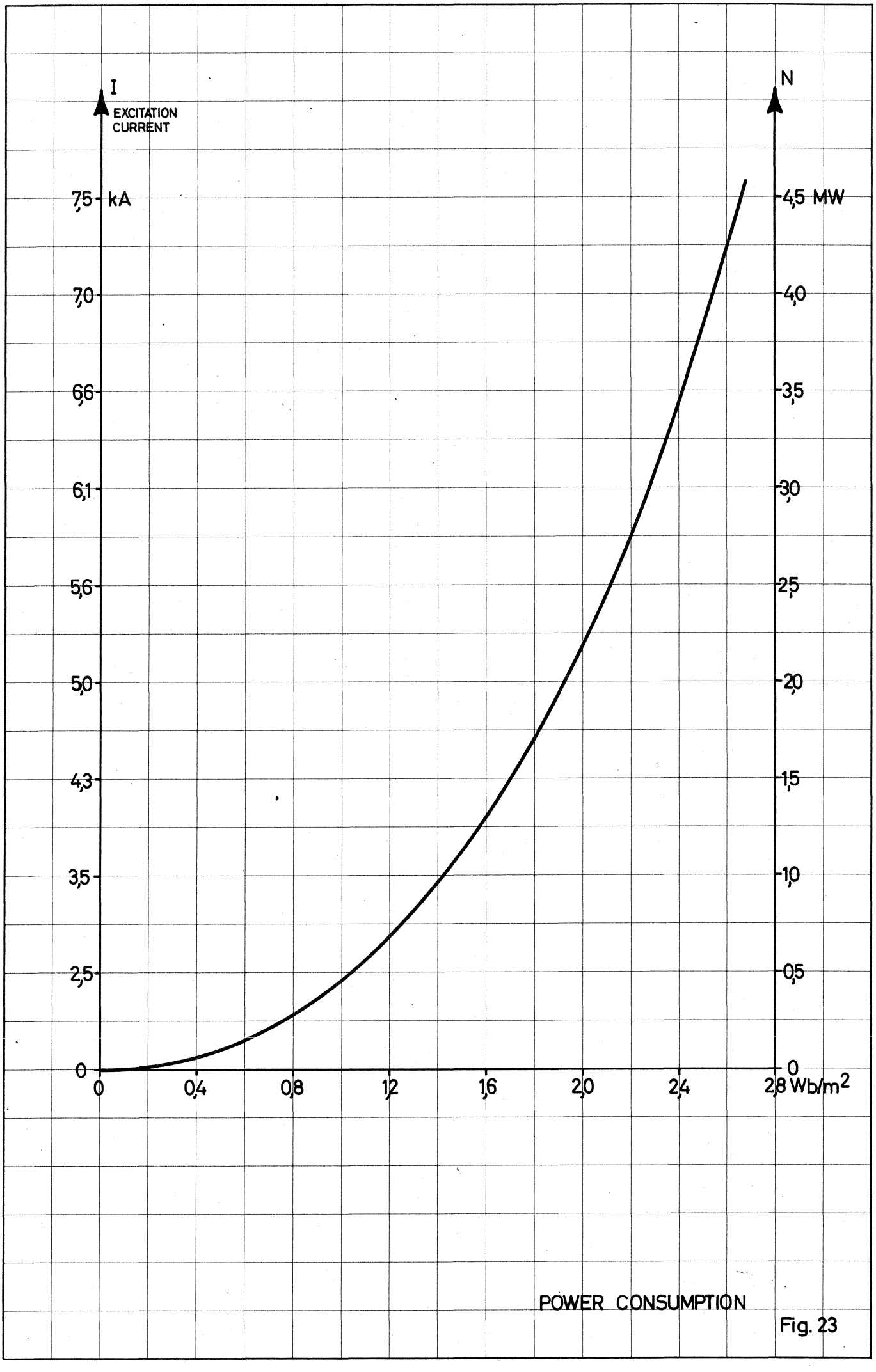

POWER CONSUMPTION

Fig. 23

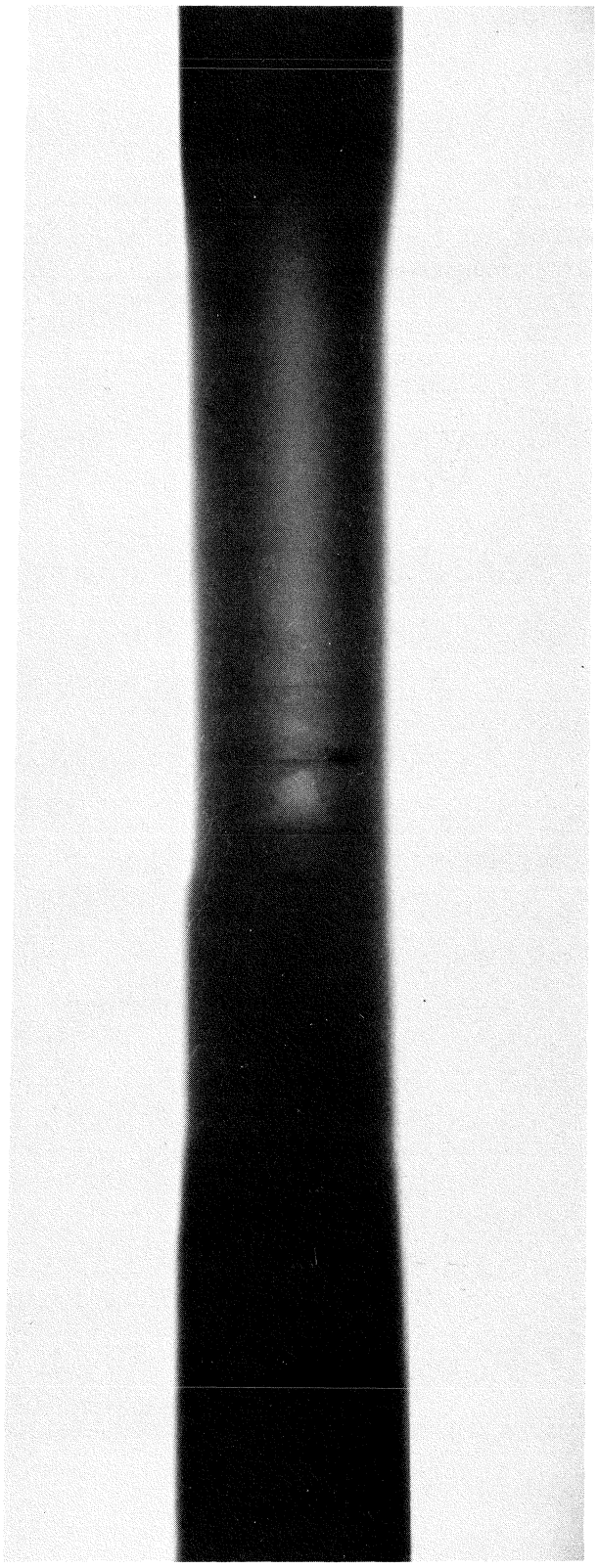

X-RAY PHOTOGRAPH OF BRAZED JOINT OF COIL CONDUCTOR

Fig. 24

TERMINAL BOX

SHUNT
10000A
500mV

AIMANT

RESISTANCES
Ø 6 – 0,16 Ω

ECLATEUR
2 KV

CABLES(~100m)
40 x 240 mm²

~ 3 Kg/cm²

EAU DEMINERALISEE
~100 m³/h 10÷25Kg/cm²

G1 G2 G3 G4

3 GENERATRICES
DE 2500A, 600V

VOLTMETRE DIGITAL
REGULATEUR
DE COURANT

VOLTMETRE
DIGITAL

CONTROLE A
DISTANCE

CIRCUITS DE
CONTROLE ET
DE PROTECTION

Thermo. Ni DEGUSSA
100 Ω a 0°c coef.de temp. $3,85 \times 10^{-3}$

Controleur de debit ELETTA
40 ÷ 80 L / mn

Thermo contact KLIXON
77 ± 3°c ÷ 71 ± 3°c

Manometre a contact

Protection contre les
surtensions

Indicateur de fuite d'eau

BUBBLE CHAMBER 1,1 m³

211.105.3

ELECTRICAL CIRCUIT DIAGRAM

Fig. 25

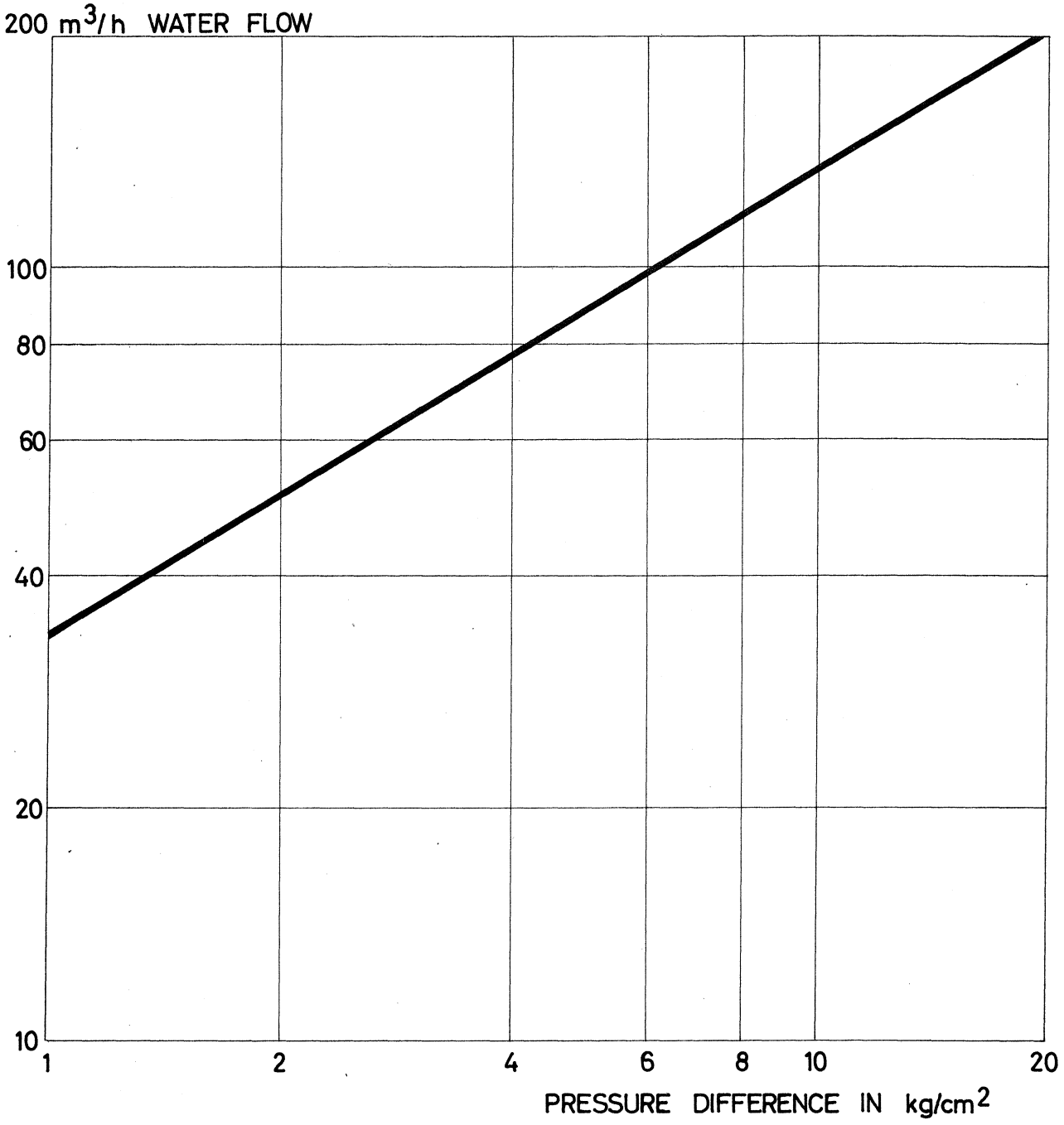

COOLING WATER FLOW

Fig. 26